Thesis for the Degree of Master of Engineering

Synthesis, Characterization and Photovoltaic Properties of Novel Alternating Copolymers Including Quinoxaline with Fluoro Group

By

Hyo Il Choi

Department of Industrial Chemistry

The Graduate School

Pukyong National University

August 2013

Synthesis, Characterization and Photovoltaic Properties of Novel Alternating Copolymers Including Quinoxaline with Fluoro Group

(유기태양전지에 적용 가능한 Fluoro 그룹을 포함하는 Quinoxaline 을 기초로 한 새로운 교대공중합체들의 합성 및 특성)

Advisor: Prof. Youngeup Jin

by
Hyo Il Choi

A thesis submitted in partial fulfillment of the requirements
for the degree of

Master of Engineering

in Department of Industrial Chemistry, The Graduate School,
Pukyong National University

August 2013

Synthesis, Characterization and Photovoltaic Properties of Novel Alternating Copolymers Including Quinoxaline with Fluoro Group

A dissertation
by
Hyo Il Choi

Approved by:

(SeongSoo Park)

(GunDae Lee)

(Youngeup Jin)

August 23, 2013

Contents

Contents ……..……..……... I

Abstract …… ……...…….……...VI

Chapter I. Introduction……..…. 1

I-1. The Background of Organic Photovoltaics (OPVs) ……..…. 1

I-2. Organic photovoltaic materials and devices……....…. 6

I-3. Progress in design, synthesis, and control of materials……... 14

I-3-1. Low-bandgap polymer design …….……..... 14

I-3-2. Push–pull conjugated polymers …….…..…. 16

I-3-3. Single-layer devices …….……...……. 18

I-3-4. Tandem devices …….……. 20

Chapter II. Results and Discussion ……. 24

II-1. Synthesis and Characterization ..…… 24

II-1-1. Preparation of monomer ...……24

II-1-1-1. Preparation of 5,8-Dibromo-6,7-difluoro-2,3-dihexylquinoxaline.24

II-1-1-2. Preparation of 5,8-bis(5-bromothiophen-2-yl)-6,7-difluoro-2,3-dihexylquinoxaline……26

II-1-1-3. Preparation of 4,4-bis(2-ethylhexyl)-4H-cyclopenta[1,2-b:5,4-b'] Dithiophene……...27

II-1-1-4. Preparation of 2,6-bis(trimethyltin)-4,8-bis(2-octyloxy)benzo[1,2-*b*:3,4-*b'*]dithiophene……...28

II-1-1-5. Preparation of 4,4-dioctyl-2,6-bis(trimethylstannyl)-4H-silolo[3,2-b:4,5-b']dithiophene……...30

II-1-1-6. Preparation of 2,2'-(9,9-bis(2-ethylhexyl)-9H-fluorene-2,7-diyl)bis(4,4,5,5-tetramethyl-1,3,2-dioxaborolane)……31

II-1-1-7. Preparation of 9-(heptadecan-9-yl)-2,7-bis(4,4,5,5-tetramethyl-1,3,2-dioxaborolan-2-yl)-9H-carbazole……33

II-1-2. Preparation of polymer……...……35

II-1-2-1. Preparation of 5-(4,8-bis(octyloxy)-6-phenylbenzo[1,2-b:4,5-b']dithiophen-2-yl)-6,7-difluoro-2,3-dihexyl-8-phenylquinoxaline (YJ-6)……35

II-1-2-2. Preparation of 5-(4,4-bis(2-ethylhexyl)-6-methyl-4H-

cyclopenta[1,2-b:5,4-b']dithiophen-2-yl)-6,7-difluoro-2,3-dihexyl-8-methylquinoxaline(YJ-7)……...……36

II-1-2-3. Preparation of 6,7-difluoro-2,3-dihexyl-5-methyl-8-(6-methyl-4,4-dioctyl-4H-silolo[3,2-b:4,5-b']dithiophen-2-yl)quinoxaline (YJ-8)…….37

II-1-2-4. Preparation of 5-(5-(4,8-bis(octyloxy)-6-phenylbenzo[1,2-b:4,5-b']dithiophen-2-yl)thiophen-2-yl)-6,7-difluoro-2,3-dihexyl-8-(5-phenylthiophen-2-yl)quinoxaline (YJ-9)…….38

II-1-2-5. Preparation of 5-(5-(9,9-bis(2-ethylhexyl)-7-phenyl-9H-fluoren-2-yl)thiophen-2-yl)-6,7-difluoro-2,3-dihexyl-8-(5-phenylthiophen-2-yl)quinoxaline (YJ-10)…….....39

II-1-2-6. Preparation of 2-(5-(6,7-difluoro-2,3-dihexyl-8-(5-phenylthiophen-2-yl)quinoxalin-5-yl)thiophen-2-yl)-9-(heptadecan-9-yl)-7-phenyl-9H-carbazole (YJ-11)……....40

II-2. Characterization of the Polymers …… 41

II-3. Optical Properties of the Polymer…… 43

II-4. Electrochemical Properties of the Polymer…….…… 46

II-5. Photovoltaic Properties of the Polymer…… 49

Chapter III. Conclusions……..…… 53

Chapter IV. Experimental…… 54

IV-1. Synthesis of acceptor monomer……...56

IV-1-1. Synthesis of 2,3-Difluoro-1,4-bis-(trimethylsilyl)benzene (2)…….56

IV-1-2. Synthesis of 1,4-dibromo2,3-Difluoro-benzene (3)……..56

IV-1-3. Synthesis of 1,4-dibromo-2,3-difiuoro-5,6-dinitro-benzene (4)…...57

IV-1-4. Synthesis of 3,6-dibromo-4,5-difluorobenzene-1,2-diamine (5)…..57

IV-1-5. Synthesis of Tetradecane-7,8-dione (6)……58

IV-1-6. Synthesis of 5,8-Dibromo-6,7-difluoro-2,3-dihexylquinoxaline (9)23

IV-2. Synthesis of acceptor monomer……...59

IV-2-1. Synthesis of 6,7-difluoro-2,3-dihexyl-5,8-di(thiophen-2-yl) quinoxaline (12)……60

IV-2-2. Synthesis of 5,8-bis(5-bromothiophen-2-yl)-6,7-difluoro-2,3-dihexylquinoxaline (13)……30

IV-3. Synthesis of donor monomer……61

IV-3-1. Synthesis of Di-3-thienylmethanol (16)……61

IV-3-2. Synthesis of Di-3-thienylmethane (17)……61

IV-3-3. Synthesis of Bis(2-bromothien-3-yl)methane (18)……...62

IV-3-4. Synthesis of 4H-Cyclopenta[2,1-b:3,4-b(]dithiophene (19)…….63

IV-3-5. Synthesis of 4,4-Di(2-ethtylhexyl)-4H-cyclopenta[2,1-b:3,4-b(]dithiophene (20)……63

IV-4. Synthesis of donor monomer……64

IV-4-1. Synthesis of thiophene-3-carbonyl chloride (22)……..64

IV-4-2. Synthesis of *N,N*-diethylthiophene-3-carboxamide (23)……..64

IV-4-3. Synthesis of 4,8-dihydrobenzo[1,2-*b*:4,5-*b′*]dithiophen-4,8-dione (24) ……65

IV-4-4. Synthesis of 4,8-Bis(2-octyloxy)benzo[1,2-*b*:3,4-*b*]dithiophene (25)……66

IV-4-5. Synthesis of ,6-Bis(trimethyltin)-4,8-bis(2-octyldodecyloxy)benzo[1,2-*b*:3,4-*b′*]dithiophene (26)……..67

IV-5. Synthesis of donor monomer……68

IV-5-1. Synthesis of 3,3’-Dibromo-2,2’-bithiophene (28)……68

IV-5-2. Synthesis of 3,3’-Di-n-octylsilylene-2,2’-bithiophene (29)……..68

IV-5-3. Synthesis of 5,5’*Bis*(trimethylstannyl)-3,3’-Di-n-dodecylsilylene-2,2’-bithiophene (30)……69

IV-6. Synthesis of donor monomer……70

IV-6-1. Synthesis of 2,7-dibromofluorene (32)……70

IV-6-2. Synthesis of 2,7-Dibromo-9,9'-bis(2-ethylhexyl)fluorene (33)……71

IV-6-3. Synthesis of 2,2'-(9,9-Bis(n-propyl)-fluoren-2,7-diyl)-bis[4,4,5,5-tetramethyl-[1,3,2]dioxaborolane] (34)……72

IV-7. Synthesis of donor monomer……73

IV-7-1. Synthesis of 4,4'-Dibromo-2-nitrobiphenyl (36)……...73

IV-7-2. Synthesis of 2,7-Dibromocarbazole (37)……..74

IV-7-3. Synthesis of octylmagnesium bromide (39)……74

IV-7-4. Synthesis of Heptadecan-9-ol (40)……75

IV-7-5. Synthesis of 9-Heptadecane p-toluenesulfonate (41)……...76

IV-7-6. Synthesis of 2,7-Dibromo-9-(heptadec-9-yl)carbazole (42)…….76

IV-7-7. Synthesis of 2,7-Bis(4’,4’,5’,5’-tetramethyl-1’,3’,2’-dioxaborolan-2’-yl)-*N*-9”-heptadecanylcarbazole (43)……...77

IV-8. Synthesis of polymer……78

IV-8-1. Synthesis of Poly-(5-(4,8-bis(octyloxy)-6-phenylbenzo[1,2-b:4,5-b']dithiophen-2-yl))-6,7-difluoro-2,3-dihexyl-8-phenylquinoxaline (YJ-6)……78

IV-8-2. Synthesis of 5-(4,4-bis(2-ethylhexyl)-6-methyl-4H-cyclopenta[1,2-

b:5,4-b']dithiophen-2-yl)-6,7-difluoro-2,3-dihexyl-8-methylquinoxaline(YJ-7)……..79
IV-8-3. Synthesis of 6,7-difluoro-2,3-dihexyl-5-methyl-8-(6-methyl-4,4-dioctyl-4H-silolo[3,2-b:4,5-b']dithiophen-2-yl)quinoxaline (YJ-8)...79
IV-8-4. Synthesis of 5-(5-(4,8-bis(octyloxy)-6-phenylbenzo[1,2-b:4,5-]dithiophen-2-yl)thiophen-2-yl)-6,7-difluoro-2,3-dihexyl-8-(5-phenylthiophen-2-yl)quinoxaline (YJ-9)……...80
IV-8-5. Synthesis of 5-(5-(9,9-bis(2-ethylhexyl)-7-phenyl-9H-fluoren-2-yl)thiophen-2-yl)-6,7-difluoro-2,3-dihexyl-8-(5-phenylthiophen-2-yl)quinoxaline (YJ-10)……81
IV-8-6. Synthesis of 2-(5-(6,7-difluoro-2,3-dihexyl-8-(5-phenylthiophen-2-yl)quinoxalin-5-yl)thiophen-2-yl)-9-(heptadecan-9-yl)-7-phenyl-9H-carbazole (YJ-11)……..81

References……....83

유기태양전지에 적용 가능한 Fluoro 그룹을 포함하는 Quinoxaline 을 기초로 한 새로운 교대공중합체들의 합성 및 특성

최 효 일

부경대학교 대학원 공업화학과

요 약

본 논문은 유기 발광소자와 고분자 태양전지의 효율을 향상시키기 위한 활성층 내 새로운 공액 고분자 개발을 연구한 결과이다. 고갈되어가는 화석연료를 대처할 수 있는 많은 대체에너지 자원 중에서 유기물을 이용하는 유기태양전지는 다른 태양전지들에 비해 경제성과 제작용이성에서 뛰어나 가장 유망한 차세대 태양전지로 고려되어 최근 국내외에서 많은 연구가 이루어지고 있다. 낮은 밴드갭을 가지는 전도성 고분자를 이용한 유기태양전지는 흡광 계수가 높아 얇은 박막으로도 태양빛을 충분히 흡수할 수 있어 얇은 소자 제작이 가능, 가벼우며, 구부릴 수 있으며, 대면적의 박막으로 만들 수 있는 장점으로 특히 신재생에너지 소재로 주목 받고 있다.

Polymer solar cells 의 가장 대표적인 기법 Bulk Heterojucntion D-A system 에서 acceptor 로 사용 되는 5,8-Dibromo-6,7-difluoro-2,3-dihexylquinoxaline 유도체는 높은 전공 이동성과 낮은 HOMO 에너지 값을 가지게 함으로써 작은 band gap 을 밴드갭을 나타낸다. Donor 물질은 bis(trimethyltin)-4,8-bis(2-octyloxy)benzo[1,2-*b*:3,4-*b*']dithiophene, 4,4-bis(2-ethylhexyl)-4H-cyclopenta[1,2-b:5,4-b']dithiophene, 4,4-dioctyl-4H-silolo[3,2-b:4,5-b']dithiophene, 2,7-dibromo-9,9-bis(2-ethylhexyl)-9H-fluorene, 2,7-dibromo-9-(heptadecan-9-yl)-9H-carbazole 를 사용하여 Stille, Suzuki 중합으로 고분자를 합성하였다. 이를 분자량, 열적 안정성, UV-vis 흡수 등을 측정을 통하여 고분자의 특성을 살펴보았다.

Chapter I. Introduction

I-1. The Background of Organic Photovoltaics (OPVs)

Organic photovoltaics(OPVs) have thus been regarded as one of the most bright approaches to solve these pressing issues. Inorganic solar cells are the most mature photovoltaic technology to date with a high power conversion efficiency (PCE) of more than 25%.[1] Nonetheless, the high cost of Inorganic solar cells has limited their wide spread commercialization. Alternatively, Organic photovoltaics(OPVs) have been rapidly developed as one of the most bright candidates for low-cost solar cells, due to their possibility of fabricating large-scale and flexible solar cells by solution processing. The most widely utilized device structure of PSCs involves the concept of bulk heterojunctions (BHJs), where a nanoscale phase separated blend of conjugated polymer donor and fullerene derivative acceptor was sandwiched between transparent indium tin oxide (ITO) and a metal electrode. Both conventional and inverted device architectures were developed for PSCs (see Fig I-1). In conventional devices, ITO and a low work- function metal were used to collect holes and electrons, respectively, while modified ITO and a high-work-function metal were used as the electron-collecting electrode and the hole-collecting electrode, respectively, for inverted devices. The fundamental operating principle of BHJ-PSCs for both conventional and inverted devices is the photo-induced charge transfer between conjugated polymer donors and fullerene derivative acceptors. Generally, the energy conversion from light energy to electrical energy experienced five fundamental steps: 1) harvesting of photons by chromophores (donor or acceptor) to generate excitons, 2) diffusion of the excitons to the interface of the p-n

junction, 3) dissociation of the excitons into free charge carriers, 4) transportation of the free charge carriers towards the corresponding electrodes, and 5) charge collection at electrodes.

In recent years, significant advances in PCEs of BHJ-PSCs have been achieved, benefiting from both material developments and device technologies.[2,3] From a materials point of view, the development of donor polymers plays a more critical role in the recent progresses of BHJ-PSCs, due to the fact that the choice of acceptor materials is limited and actually, most state-of-the-art BHJ-PSCs utilized (6,6)-phenyl-C61-butyric acid methyl ester (PC61BM, see Scheme 1) or (6,6)-phenyl-C71-butyric acid methyl ester (PC71BM, see Scheme 1) as acceptor phase. In principle, an ideal donor polymer for high performance BHJ-PSCs should possess the following properties simultaneously: 1) appropriate solubility and miscibility with acceptors to form the desired bi-continuous penetrating network in the active layers, 2) well-matched energies of the frontier levels between the polymer and acceptor (PC61BM or PC71BM) to guarantee sufficient driving force for efficient charge separation while maintaining a high open-circuit voltage (Voc), 3) broad absorption spectra coupled with a high extinction coefficient to match with the solar terrestrial radiation in the range of 300–1500 nm, with maximal flux at 690 nm, and to harvest as much solar photons, and 4) high hole mobility to efficiently transport charge carriers to the electrode. To satisfy these criteria, a large amount of new polymers have been developed by synthetic chemists as donor materials for BHJ-PSCs and, encouragingly, dramatic advances in the PCEs for BHJ-PSCs were thus achieved.[4]

In early studies, homopolymers such as poly(2-methoxyl- 5-((20-ethylhexyl)oxy)-1,4-phenylenevinylene) (MEH-PPV), poly(2-methoxyl-5-((30,70-dimethyloctyl)oxy)-1,4-phenylenevinylene) (MDMO-PPV), and regioregular polythiophene derivatives (such as poly-(3-hexylthiophene) (P3HT)) (see Scheme 1) were usually applied as donor materials in BHJPSCs. However,

the solar cell devices using these polymers usually delivered limited PCEs, which retarded the practical application of these materials in BHJ-PSCs. The relatively low PCEs of solar cells based on these polymers have been attributed to their narrow absorption spectra and non-ideal frontier molecular orbitals, which limited the short circuit current (Jsc) and Voc, respectively, in the resulting BHJ-PSCs. Therefore, the development of new photovoltaic materials with smaller optical band gaps (Eg) and suitable highest occupied molecular orbital (HOMO) and lowest unoccupied molecular orbital (LUMO) energy levels is crucial to further improve the PCEs of BHJPSCs. Push–pull conjugated polymers, or the so-called donor– acceptor (D–A) alternating conjugated polymers were thus extensively developed and have dominated the library of donor materials for PSCs because their intrinsic optical and electronic properties, including light-absorption ability and energy levels, can be tuned readily by controlling the intramolecular charge transfer (ICT) from donor unit to acceptor unit. Encouragingly, a PCE over 7% is now a normality in the research field of BHJPSCs and a record-high PCE of 8.5% was also achieved, mainly due to the successfully development of push–pull narrow bandgap (NBG) conjugated polymers.[5] The principle of band gap and energy level manipulation by ICT interaction in push–pull conjugated polymers can be easily understood by molecular orbital theory. As depicted in Fig I-2, the HOMO of the donor segment will interact with that of the acceptor segment to generate two new occupied molecular orbitals after covalent bond connection of two different moieties, one of them is higher and the other one is lower than the two initial HOMOs before molecular orbital hybridization. Two new unoccupied molecular orbitals would also be generated in a similar manner after molecular orbital hybridization, where one is lower and the other is higher than the two initial LUMOs of the two moieties. Hence the overall effect of this redistribution of frontier molecular orbitals is the formation of a higher-positioned HOMO and a lower-positioned LUMO in the whole conjugated main chain, and this

accordingly leads to the narrowing of the band gap. Clearly, the rational selection of building blocks, including both donor units and acceptor units is critical to the realization of the well-defined control of the photophysical properties and frontier molecular orbital energy levels of the resulting copolymers to meet the requirements for BHJ-PSC applications. Therefore, various aromatic heterocycles were exploited or used as building blocks to develop highly efficient donor polymers for BHJ-PSC applications based on the push–pull design. Moreover, the fine tailoring of the structure (such as incorporation of functional groups onto the backbone, the selection of alkyl side chains, end capping and so forth) is also critical for obtaining high-performing donor polymers, although the nature of the conjugated backbone dominated the intrinsic electronic properties (especially band gaps, energy levels, and charge carrier transporting ability). It should be pointed out that conjugated polymers which consist of alternating electron-rich building blocks but can provide stable quinoidal structures are another class of state-of the- art donor polymers for BHJ-PSCs, aside from push–pull conjugated polymers.[6] BHJ-PSCs based on this kind of material even delivered unprecedented PCEs higher than 8.0% after meticulous device optimization. In this feature article, we will briefly summarize the important advances of push–pull conjugated polymers, which were used as the donor phase for high-efficiency BHJ-PSCs. Our emphasis will be placed mainly on how the materials' chemical structures influenced their properties, such as the absorption spectra, energy levels, mobilities and photovoltaic behaviors, based on the recently reported literature. Although several published reviews have already summarized the major classes of conjugated polymer employed as donors in BHJ-PSCs. For more information on the topic of donor polymers in BHJ-PSCs.[7]

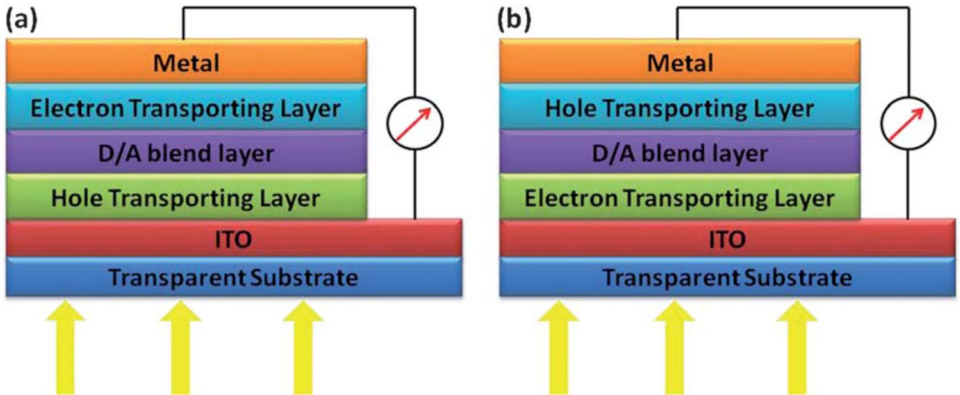

Fig I-1. Device structures of BHJ-PSCs with (a) conventional and (b) inverted configurations. [7]

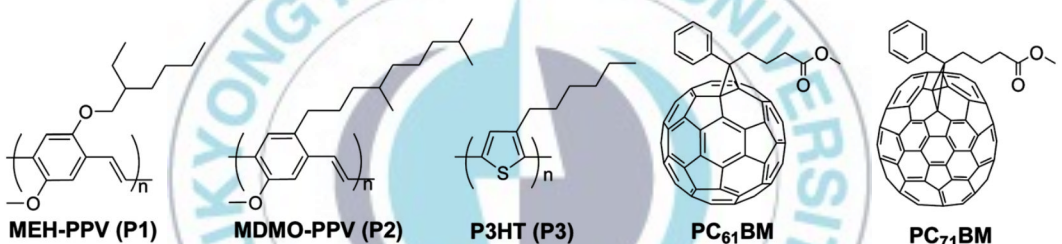

Scheme I-1. The chemical structures of MEH-PPV, MDMO-PPV, P3HT, PC61BM and PC71BM. [7]

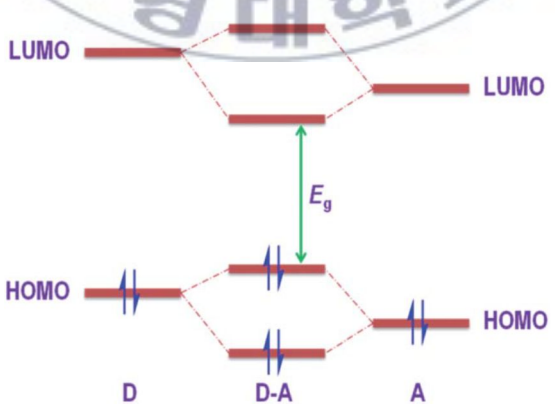

Fig I-2. Molecular orbital interactions of donor and acceptor units, resulting in a narrowing of the band gap in push–pull conjugated copolymers.[7]

I-2. Organic photovoltaic materials and devices

Organic semiconductors are carbon based molecular materials, including both polymers of molecular weight 10 – 100 kDa and "small" molecules of molecular weight of 100 – 1000, based around a backbone of sp2 hybridized carbon atoms. Electronic interactions between pz orbitals on neighboring C atoms constitute a π electronic system, with orbitals delocalized over conjugated segments several nanometers in size. The energy gap between the highest of the filled π orbitals, known as the highest occupied molecular orbital or HOMO, and the lowest unoccupied molecular orbital or LUMO is typically in the range 1 – 3 eV, much smaller than the gap between filled and unfilled levels in a saturated (not π conjugated) carbon based molecule, and, importantly, accessible to visible light. The delocalization of the π orbitals means that charges, which may be generated electrically or optically, are weakly bound and free to travel along and between molecules by a hopping process. The disorder in molecular packing also means that the energies of electronic states on different molecules may be different, leading to a distribution in the HOMO and LUMO energies. The states with the lowest lying LUMO energies and highest lying HOMO energies may act as charge traps. As a result of both the weak electronic interaction between conjugated segments and the charge traps, the resulting charge mobilities are in the range 10-6 to 1 cm2/Vs and much lower than those found in crystalline inorganic semiconductors.

For photovoltaic applications, the most important feature that distinguishes organic from inorganic semiconductors is the fact that excited states are localized. When a photon is absorbed by an organic semiconductor it generates a neutral excited state or exciton that is localized on a single molecule or a single conjugated segment, so within a volume of a few nm^3. This spatial confinement,

together with the low dielectric permittivity (ε ≈ 3 – 4) of organic semiconductors makes it difficult for the exciton to dissociate into a separated electron and hole, since the Coulomb energy binding such localized charges is high (~1 eV) compared to kBT. In comparison, the exciton in a crystal of silicon has a diameter of tens of nm and a binding energy of around 0.1 eV, allowing charge pairs to be generated spontaneously at room temperature. As a result, the exciton in an organic semiconductor tends not to dissociate into charges but rather to decay to the ground state within a few ns, sometimes releasing light. In organic solar cells and photodiodes, this problem is solved by introducing a second molecular component (the electron acceptor) that has a higher affinity for electrons, such as a fullerene. Then when an exciton is photogenerated within the first, donor phase but close to this second type of molecule, the electron is attracted to the higher affinity molecule by the free energy difference, and the lost exciton binding energy is provided by the difference in free energies ΔG between the exciton and the charge separated state, Fig I-3.

Once the charges are located on different types of molecule, the electron on an acceptor molecule and the hole remaining on a donor molecule, the charges at first form a geminate pair in which they are held by Coulombic forces. Once this pair is separated, the two types of charge may travel through the respective phase, and may be collected when they encounter a low resistance contact to the external circuit. This requires that the two phases percolate through the medium.

The requirements for photocurrent and photovoltage generation in an organic donor-acceptor device are thus as follows:

• Visible light must be absorbed in the donor or acceptor material or both.

• The width of domains of pure donor or acceptor material should be shorter than the distance an exciton diffuses before decaying (< ~10 nm), in order for most photogenerated excitons to dissociate, i.e., the two components should be sufficiently well mixed.

• Both phases should form continuous percolating networks that connect the bulk of the film to the electrodes.

• The electrodes should be electronically different, such that electrons are preferentially collected at one and holes at the other, in order to provide a direction for the photocurrent. Such selectivity can be achieved using one high and one low work function electrode.

A typical device has the layer structure (Fig I-4): Glass / indium tin oxide (ITO) / polyethylenedioxythiophene: polystyrene sulphonate (PEDOT:PSS) / photoactive blend layer / cathode interlayer (such as Ca or LiF / Al) where the PEDOT:PSS is a doped conducting polymer that is used to raise the work function of the bottom electrode in order to accept holes, and the cathode interlayer (usually a low work function metal) is used to lower the work function of the top electrode to accept electrons. The photoactive layer is typically 100 – 200 nm thick while other layers are some 50 – 100 nm. The same layer structure may be deposited on a transparent flexible substrate such as polyethylene terephthalate (PET) instead of glass. A similar structure with inverted polarity such as: Glass / ITO / metal oxide / photoactive blend layer / PEDOT:PSS / Ag is now being widely studied, mainly for the reason that no evaporated metal layers are required. A low work function metal oxide such as TiO2 or ZnO can be cast from solution and the top silver contact can be applied as a paste, allowing for production in a roll to roll process.[8]

A typical current voltage characteristic of the best studied variety of organic solar cell, a blend of poly-3-hexylthiophene (P3HT) and the fullerene derivative [6,6]phenyl C61 butyric acid methyl ester (PCBM) is shown in Fig I-5 (b) (black line), together with data for higher performing materials systems. In comparison with inorganic solar cells, OPV devices show a lower circuit current density (Jsc) and fill factor (FF) than inorganic devices while open circuit voltage (Voc) values are comparable to those of inorganic solar cells. However, in comparison to

inorganic PV cells, the value of e·Voc (where e is electronic charge) is lower than the optical energy gap of the light absorbing materials by a larger margin, indicating that more of the electrochemical potential generated by the light is lost.

The differences in comparison with inorganic solar cells can be rationalized in terms of the properties of organic semiconductor materials. In the case of Jsc, the lower value in OPV is mainly due to the larger optical gap of the organic semiconductors used, typically 1.5 to 2 eV compared to 1.1 eV for silicon. Thus there is a need for stable organic semiconductors with light absorption further into the infrared, however, it should be stressed that the optimum energy gap in the standard solar spectrum is larger for a hetero junction solar cell than for a homo junction such as silicon, because some energy has to be paid for charge separation. In addition, the value of Jsc in OPV is strongly influenced by optical interference effects in the thin multilayered structure.

Fill factor is controlled largely by the changing competition between photocurrent generation and charge recombination as the bias between the electrodes varies. Recombination processes are commonly distinguished as geminate and non-geminate (also referred to as "bimolecular"). Geminate recombination refers to the recombination of nascent charge pairs soon after (within ~100 ns) exciton dissociation. It is an issue unique to OPV devices that results from the difficulty of separating dissociated charges and it may be assisted by an electric field, leading to a dependence on applied bias. Non-geminate recombination refers to the recombination of separated charges and is important in OPV because the low charge mobilities and interpenetrating phases mean that opposite charges are likely to encounter each other before they escape through the electrodes. For both geminate and bimolecular processes, the competition between charge generation or collection and recombination is influenced by the internal microstructure of the blend.

Although Voc is limited by the energy levels of separated charges, i.e., the

HOMO of the donor and LUMO of the acceptor, Voc and FF can both also be limited by imperfect contacts with the electrodes, for example, due to poor energetic matching or resistive interfacial layers.[9,10] This affects OPV in particular because conjugated polymers cannot readily be doped, and so the electrochemical potential at the electrode is influenced by the electrode work function and the degree of charge transfer with the organic semiconductor, rather than only by the semiconductor HOMO and LUMO energies.

These features have led to some common goals in the development of new materials for OPV, namely:

• A lower polymer optical gap to raise Jsc.

• Higher ionization potential donors and lower electron affinity acceptors to raise Voc and reduce the energy loss during charge separation.

• Self organizing materials with the capability to control blend microstructure.

• The development of electrode materials with work function matched to the new semiconductors as well as transparency and conductivity.

These themes have been the focus of intense research and have led to a steady series of efficiency increases, Fig I-5. They will be discussed in the next section.

A separate goal has been the development of efficient OPV tandem devices where two or more bulk heterojunction cells with different optical gaps are integrated into a vertical device structure. Tandems offer to raise efficiency by converting more of the absorbed photon energy into useful work and can, in principle, be made using the same multiple layer solution processing techniques used for single junction OPV devices. The relative ease of depositing multiple layers successively in a continuous process makes tandem structures very accessible for organic semiconductors. Although we have no space to review developments in OPV tandems here, we stress that an efficient tandem device is built on efficient component cells, and the principles described here for development of OPV materials and devices are equally relevant for tandems.[11]

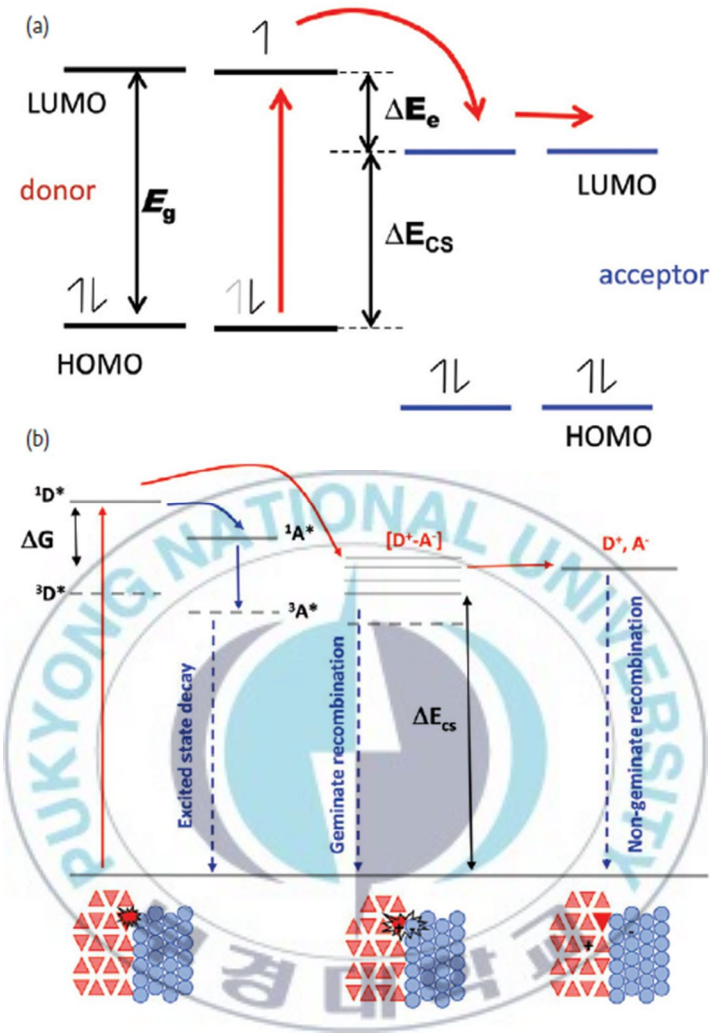

Fig I-3. (a) Schematic energy level diagram of the hetero junction between the electron donor and electron acceptor in an organic solar cell. A photon absorbed in the donor promotes an electron to the donor LUMO level. That electron may then transfer to the acceptor LUMO, and then away from the junction by hopping. The nominal driving force is the difference in LUMO energies, ΔE_e. (b) State diagram showing the total energy of the states involved in charge pair generation. From left to right, donor (singlet and triplet states), acceptor (singlet and triplet), geminate pair, charge separated state. The lower panel depicts the spatial evolution of the states at the hetero junction. Red arrows show the processes leading to photocurrent generation. Blue arrows show the loss processes of excited state decay, geminate recombination, and non-geminate recombination. [11]

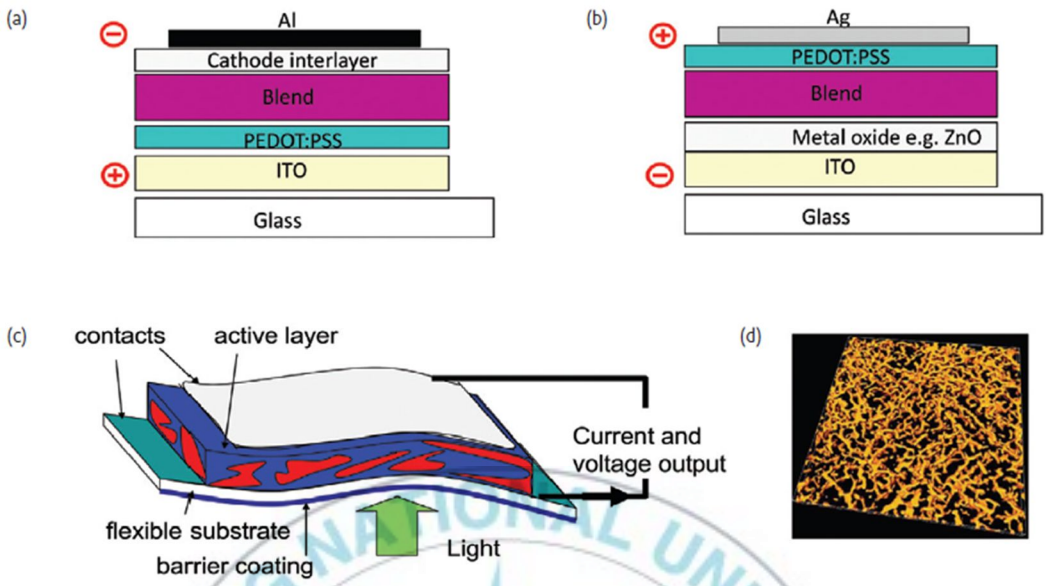

Fig I-4. Layer structure of an organic solar cell in the traditional (a) and inverted (b) polarity. (c) Schematic of the layers in an OPV module on a flexible substrate. (d) mage of the microstructure within the active layer, obtained with electron tomography. [11]

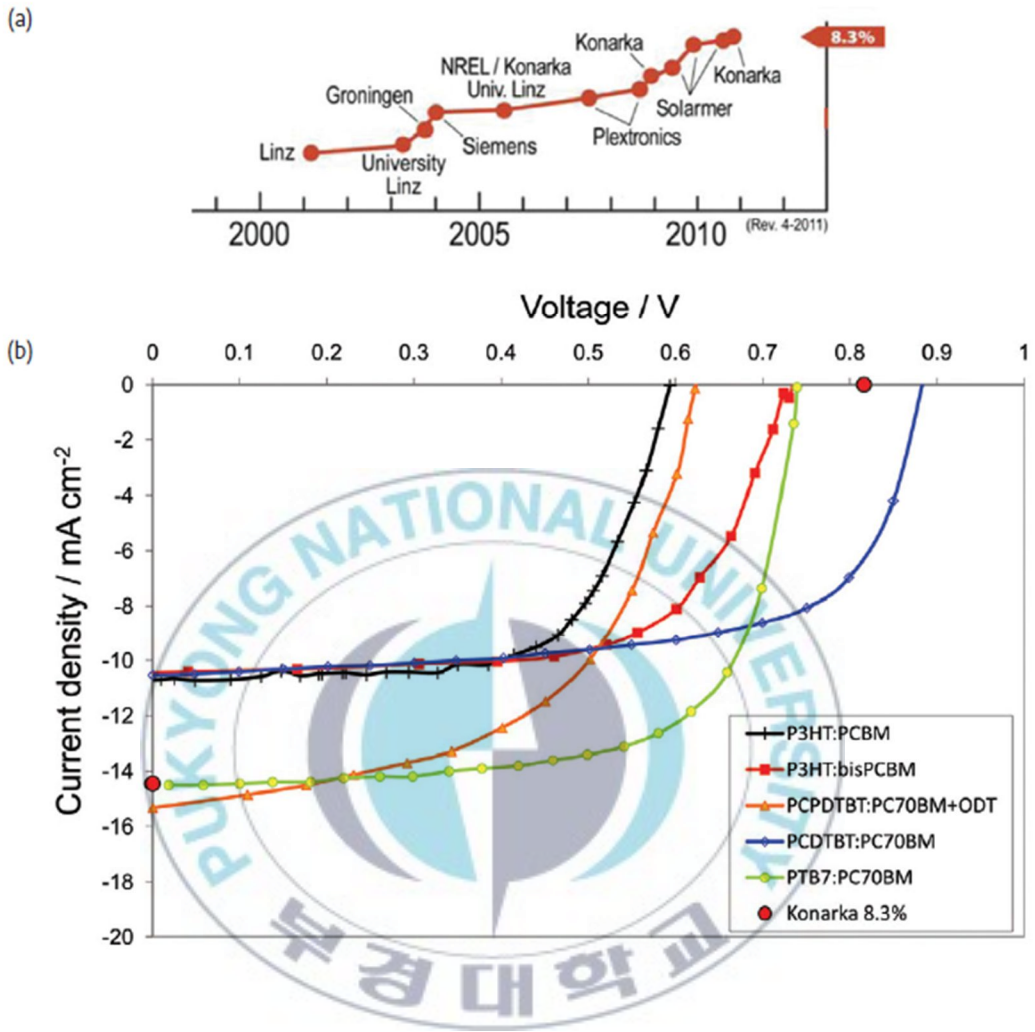

Fig I-5. (a) Evolution of the record efficiencies of polymer:fullerene solar cells. (b) Device current density – voltage characteristics for the well studied P3HT:PCBM system (black line) and several superior material combinations: P3HT with the bis adduct of PCBM (red curve); poly[2,6-(4,4-bis-(2-ethylhexyl)-4H-cyclopenta[2,1- b;3,4-b']-dithiophene)-alt-4,7-(2,1,3-benzothiadiazole)] (PCPDTBT):PC70BM (orange curve); poly[N-9-hepta-decanyl-2,7-carbazole-alt-5,5-(4,7-di-2-thienyl- 2,1,3-benzothiadiazole) (PCDTBT):PC70BM (blue curve); and Poly[[4,8-bis[(2 ethylhexyl)oxy]benzo[1,2-b:4,5-b']dithiophene-2,6-diyl][3-fluoro-2-[(2-ethylhexyl) carbonyl]thieno[3,4-b]thiophenediyl]] (PTB7):PC70BM. Also shown are the Voc and Jsc of the most efficient certified organic solar cell. [11]

I-3. Progress in design, synthesis, and control of materials

I-3-1. Low-bandgap polymer design

A number of strategies have been pursued in order to extend the absorption range of donor polymers for OPV. These include strategies aimed at extending the conjugation length of the π-conjugated segments, for example, by replacing phenyl rings with thiophene rings that help to planarize the polymer backbone through a reduced steric effect or by planarizing neighboring monomers by using a bridging atom[12]. Planarization may reduce optical gap further by enabling π-stacked aggregates to form. An alternative approach is to vary the heteroatoms in the conjugated backbone: replacing the sulphur atom in polythiophene with selenium leads to a lowered LUMO energy but unchanged HOMO, due to the influence of the heteroatom on the LUMO in this molecule. A third route, which is now widely used, is to combine electron rich (e.g., thiophene containing) and electron poor (e.g., benzothiadiazole [BT]) units in the polymer backbone in a so called 'push-pull' structure. Here, the HOMO of the copolymer is dominated by the HOMO of the electron deficient unit and the LUMO by that of the electron rich unit. The strategy is widely adopted, due to the large range of ‘push’ and ‘pull’ units that can be used and the ability to control copolymer HOMO and LUMO energies independently. Notable advances in OPV efficiency were made

using push-pull copolymers based on dithiophene - BT structures, carbazole – BT structures, and dithienobenzene - modified BT structures and diketopyrrolopyrrole - thiophene structures[13], Fig I-6. In the case of fullerenes, optical absorption in the visible is weak on account of the high symmetry of the C60 cage and resulting symmetry forbidden optical transitions. Here, optical absorption can be enhanced by replacing the symmetric C60 cage with one of lower symmetry such as C70. This leads to strong blue-green absorption by C70 fullerenes and for this reason they are routinely used with low gap polymers to complement the polymer absorption and span the visible spectrum.[11]

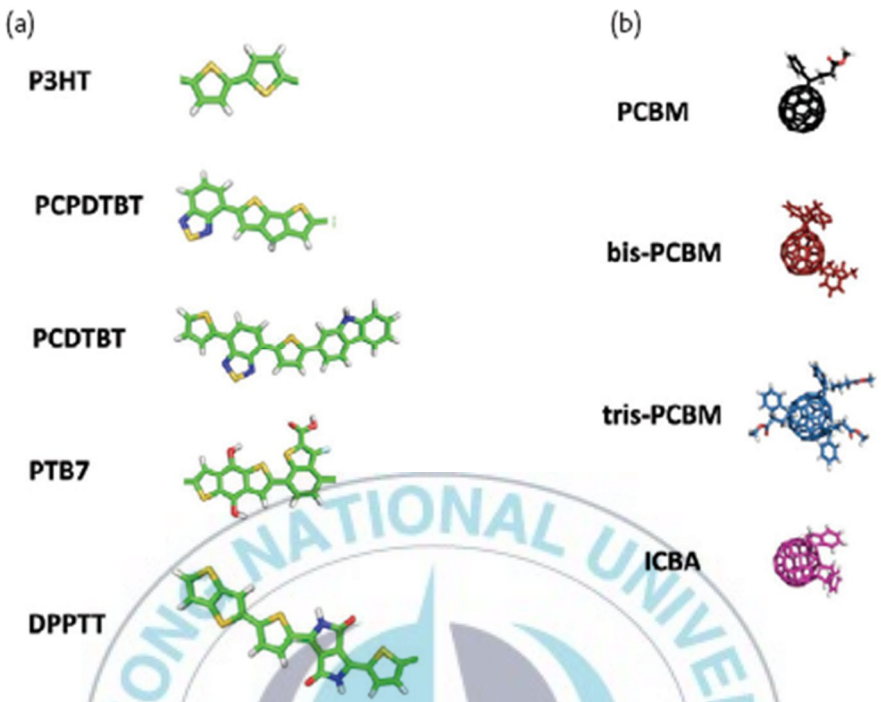

Fig I-6. (a) Chemical structures of the backbones of the polymers, P3HT, PCPDTBT, PCDTBT, PTB7 and a DPP-co-thienothiophene polymer. Side chains are omitted for clarity. (b) Chemical structures of the fullerenes, PCBM and its bis adduct and tris adducts, and a bis adduct of the indene fullerene (ICBA). [11]

I-3-2. Push–pull conjugated polymers

Push–pull conjugated polymers or the so-called 'D–A conjugated polymers', whose main chains were constructed from alternating donor units (D) and acceptor units (A), were widely developed as highly efficient donor materials in BHJ-PSCs because their light harvesting abilities and energy levels can be well tuned by controlling the photo-induced ICT from donor to acceptor units. The

intrinsic optical and electronic properties of the resulting polymers were dominated by their subunits of constructing aromatic heterocycles. Therefore, different building units have significant influence on the final photovoltaic properties of the resulting polymers. Several reviews have already comprehensively summarized the major classes of push–pull conjugated polymers employed as donors in PSCs according to the classification of subunits. In this section, we will briefly summarize several important aromatic heterocyclic subunits and their corresponding push–pull conjugated polymers in BHJ-PSC applications. Generally, fluorene, silafluorene, carbazole, benzo[1,2-b:4,5-b]-dithiophene (BDT), cyclopenta[2,1-b:3,4-b']dithiophene (CPDT),dithieno[3,2-b:2',3'-d]-silole (DTS), indacenodithiophene (IDT), etc. were used as donor units, while 2,1,3-benzothiadiazole (BT), quinoxaline, thieno[3,4-c]pyrrole-4,6-dione (TPD), pyrrolo[3,4-c]-pyrrole-1,4-dione (DPP), etc. were used as acceptor units for constructing push–pull NBG photovoltaic materials.[7]

I-3-3. Single-layer devices

Single-layer BHJ photovoltaic cells based on PBDTT-DPP blended with $PC_{71}BM$ were fabricated with a regular and an inverted configuration.[14] The optimized polymer:$PC_{71}BM$ blend ratio (by weight) was found to be 1:2 and the optimized film thickness was ~100 nm. The single-cell photovoltaic performance of PBDTT-DPP is shown in Fig I-7(a). Of the more than 300 devices that were fabricated, the best devices gave the following values: $V_{OC} \approx 0.74$ V, JSC ≈ 13.5 mA cm^{-2}, FF≈ 65%. PCE values as high as 6.5% were achieved for both regular and inverted structures; indeed, 90% of the devices gave PCE values over 6.0%. All the parameters that determine overall performance were dramatically better than those achieved using the previous low-bandgap polymer, PBDT-DPP.[15] The increase in Voc can be attributed to the deeper HOMO level, and the enhancement of Jsc and FF can be attributed to the higher hole mobility of PBDTT-DPP (the hole mobility of PBDTT-DPP:PC71BM with a 1:2 weight ratio was found to be 2.9×10^{-4} cm^2 V^{-1} s^{-1}, which is close to the pristine polymer, indicating that charge carrier transport is not disturbed by adding $PC_{71}BM$ into the polymer network). It is worth mentioning that compared to early efforts in inverted OPV devices, a very high FF (65%) is achieved here, which indicates that the interface materials have superior performance. Fig I-7(b) shows the EQE for the corresponding single-junction devices, which exhibit broad response

ranges covering 350–850 nm, with an average EQE of 47% within this region and a peak EQ of ~55%. These results indicate that the low-bandgap polymer successfully achieves high performance while maintaining a small bandgap.[16]

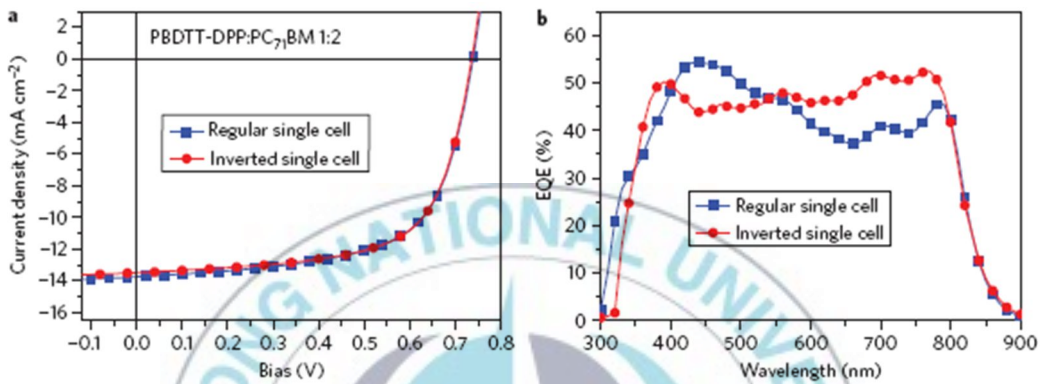

Fig I-7. J–V characteristics and EQEs of regular and inverted single-cell devices. (a) J–V characteristics of single-cell devices with regular and inverted structures under AM1.5G illumination from a calibrated solar simulator with an irradiation intensity of 100 mWcm^{-2} (about one sun). (b) EQE of the corresponding devices. Both regular and inverted single-cell devices show identical highest performances with Voc= 0.74 V, Jsc≈ 13.5 mA cm^{-2}, FF≈ 65% and PCE=6.5%. The devices exhibit a very broad response range covering 350–850 nm. [16]

I-3-4. Tandem devices

A detailed study was carried out on the tandem PSCs based on PBDTT-DPP. In our tandem structure, P3HT (a high-bandgap polymer) and the acceptor indene-C_{60} bisadduct ($IC_{60}BA$)[17] were selected as front-cell materials, and PBDTT-DPP together with the acceptor $PC_{71}BM$ were chosen as rear-cell materials. The corresponding chemical structures are shown in Fig I-8(a). In this Article, the inverted tandem structure was chosen because of its advantages of a simple, robust device fabrication process and better stability. The device structure and the corresponding energy diagram are shown in Fig I-8(b),(c). ZnO nanoparticles were used as the electron-transport material because their workfunction matches well with the acceptors and the high electron mobility.[18] PEDOT:PSS was used as the hole-transport material for P3HT, and MoO_3 was used for PBDTT-DPP because of their good workfunction aligment with the polymer and its high hole mobility. Ultraviolet photoelectron spectroscopy was used to examine the workfunctions of the ICLs, including PEDOT:PSS and ZnO (Supplementary Fig. S5). The results were in accordance with reported data. The energy difference between different layers was minimized by material selection to ensure good charge transport.

Inverted tandem solar cells were fabricated using the rear-cellspecific low-bandgap polymer PBDTT-DPP and the new device architecture. The J–V

characteristics, EQE and performance parameters of a typical device are shown in Fig I-9 and Table I-1 (EQE results measured at NREL were almost identical to those measured at the University of California, Los Angeles (UCLA)). The EQE of individual sub-cells in the tandem structure was measured using light bias, as first proposed by Burdick and Glatfelter in the 1980s for inorganic multijunction cells and more recently adopted by Kim and Janssen in organic tandem solar cells. As shown in Fig I-9(a), the front cell had a photoresponse from 300 to 600 nm, showed an EQE as high as 60% at 530 nm, and its integrated Jsc was 8.2mA cm^{-2}. The rear cell had a broad photoresponse from 300 to 850 nm, showed a maximum EQE of 47% at 770 nm, and its integrated Jsc was 8.1mA cm^{-2}. The incident light from 300 to 600 nm was strongly absorbed by the front cell, and the EQE of the rear cell in this region was much lower than that of its single-cell devices (Fig. I-7(b)); however, the rear cell can still provide enough photocurrent (8.1mA cm^{-2}) to match the current supplied by the front cell (8.2mA cm^{-2}), because the new material, PBDTTDPP, can very efficiently use the low-energy portion (from 600 to 850 nm) of the solar radiation.[16]

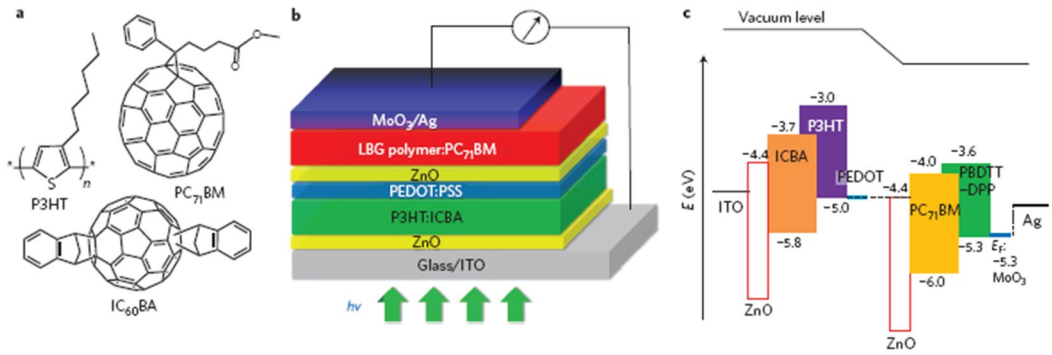

Fig I-8. Inverted tandem solar cells. (a) Chemical structures of P3HT, $IC_{60}BA$ and $PC_{71}BM$. (b) Device structure of the inverted tandem solar cell (LBG, low bandgap). (c) Energy diagram of the inverted tandem devices. [16]

	V_{OC} (V)	J_{SC} (mA cm^{-2})	FF (%)	PCE (%)
Front cell	0.85	9.56	70.2	5.7
Rear cell	0.74	13.5	65.1	6.5
Tandem (NREL)	1.56	8.26	66.8	8.6
Tandem*	1.20-1.58	6.0-7.8	52.0-67.0	4.9-6.5

Table I-1. Inverted single and tandem solar cell performance. [16]

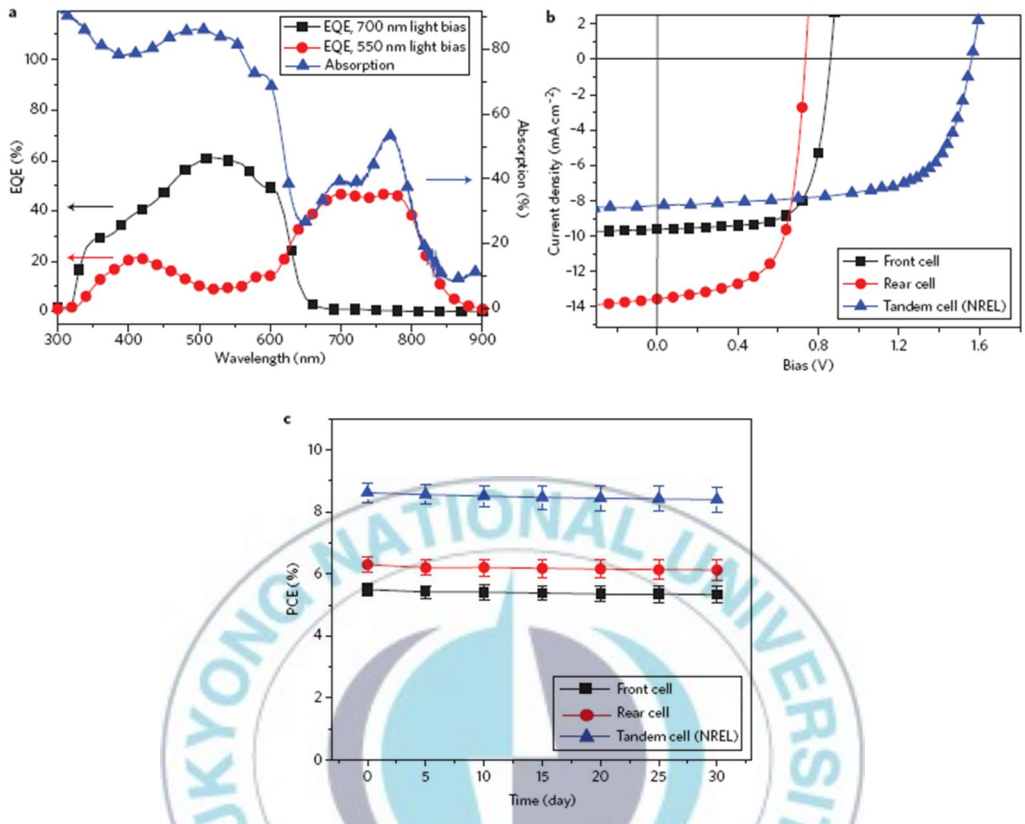

Fig I-9. Quantum efficiencies, J–V characteristics and stability of single cells and tandem cells. (a) EQEs of the inverted tandem solar cell and absorption spectrum (without metal electrode). (b) J–V characteristics of the front cell, rear cell and inverted tandem solar cell, tested at NREL using the OSMSS simulator. (c) Stability of the inverted front cells, rear cells and tandem cells. [16]

Chapter II. Results and Discussion

II-1. Synthesis and Characterization

II-1-1. Preparation of monomer

II-1-1-1. Preparation of 5,8-Dibromo-6,7-difluoro-2,3-dihexylquinoxaline

The synthetic route of difluoro-Quinoxaline **(DFQx)** is outlined in Scheme **1**. In the first step, n-butyllithium was added to a solution of di-isopropylamine in THF at -78 ℃. 1,2-difluorobenzene **(1)** and chlorotrimethylsilane were added to afford 2,3-Difluoro-1,4-bis-(trimethylsilyl)benzene **(2)**. The compound **2** was brominated by refluxing with 99% Br_2 to give 1,4-dibromo2,3-Difluoro-benzene **(3)**. The nitration of **3** in the mixture of HNO_3 and conc. H_2SO_4. The NO_2 groups of 1,4-dibromo-2,3-difiuoro-5,6-dinitro-benzene **(4)** were further reduced by $SnCl_2 \cdot 2H_2O$ to result in 3,6-dibromo-4,5-difluorobenzene-1,2-diamine **(5)**. Finally, the ring closure of compound **5** with Tetradecane-7,8-dione in the mixture of ethanol and acetic acid generated the difluoro-substituted Quinoxaline monomer **(DFQx)** in 18% yield.

Scheme 1. Synthetic route of acceptor monomer

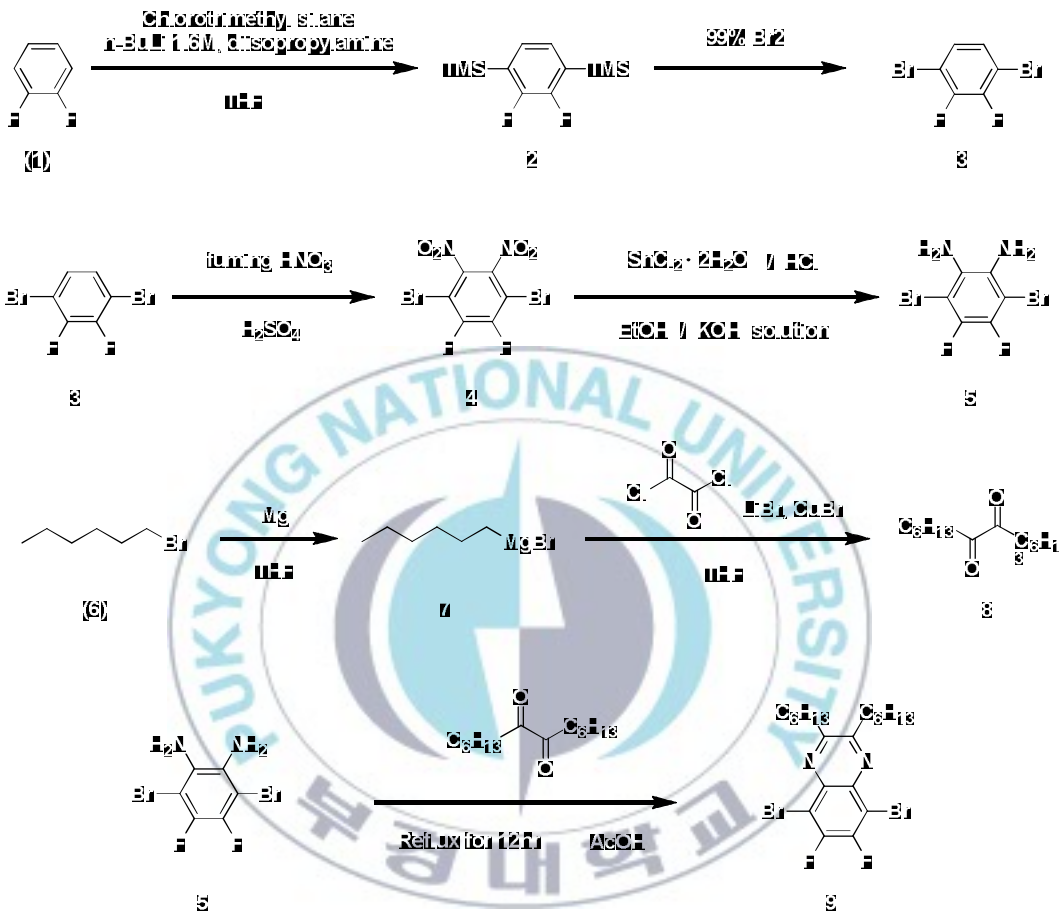

II-1-1-2. Preparation of 5,8-bis(5-bromothiophen-2-yl)-6,7-difluoro-2,3-dihexylquinoxaline

The synthetic route of 5,8-bis(5-bromothiophen-2-yl)-6,7-difluoro-2,3-dihexylquinoxaline is outlined in Scheme **2**. In the first step, thiophene in THF was added to 1.6 M n-Butyllithium in Hexane. The coupling reaction with monomer 5,8-Dibromo-6,7-difluoro-2,3-dihexylquinoxaline and monomer tributyl(thiophen-2-yl)stannane was achieved under stille coupling condition using $PdCl_2(pph)_2$. The compound **13** was brominated by NBS in THF.

Scheme 2. Synthetic route of acceptor monomer

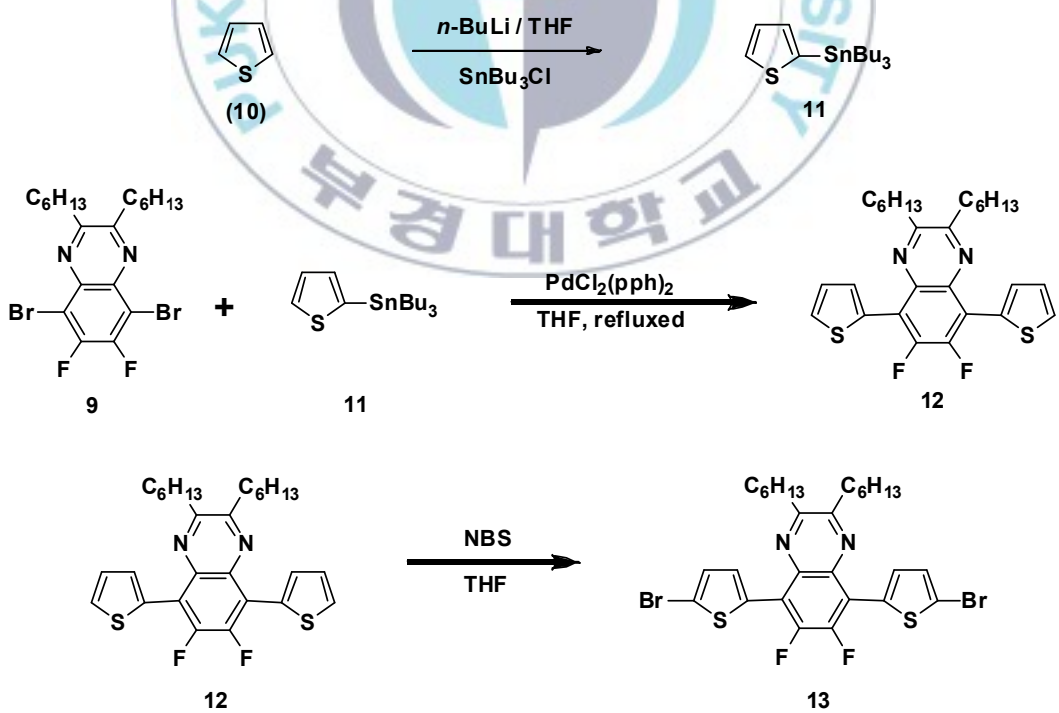

II-1-1-3. Preparation of 4,4-bis(2-ethylhexyl)-4H-cyclopenta[1,2-b:5,4-b'] dithiophene

The synthetic route of Cyclopentadithiophene(CPDT) is outlined in Scheme **3**. First, 3-bromothiophene **(14)** was lithiated and subsequently coupled with ethyl formate **(15)** to yield di-3-thienylmethanol **(16)**. Without further purification **16** was reduced with LiAlH4 to yield di-3-thienylmethane **(17)**, which could be isolated more easily than **16**. The overall yield of the first two steps is about 88%. Direct bromination of **17** with N-bromosuccinimide (NBS) proceeded selectively at the 2 and 20 positions to yield the dibrominated dithienomethane **18**. The subsequent intramolecular Ullmann coupling to 4H-cyclopenta[2,1-b:3,4-b0]dithiophene **(CPDT,19)** proceeded with microwave irradiation within 3 h at moderate yield (30%). Recrystallization from methanol gave 6 as off-white flakes. Alkylation of 6 was achieved in the presence of a base and 2-ethylhexylbromide to give **20.**

Scheme 3. Synthetic route of donor monomer

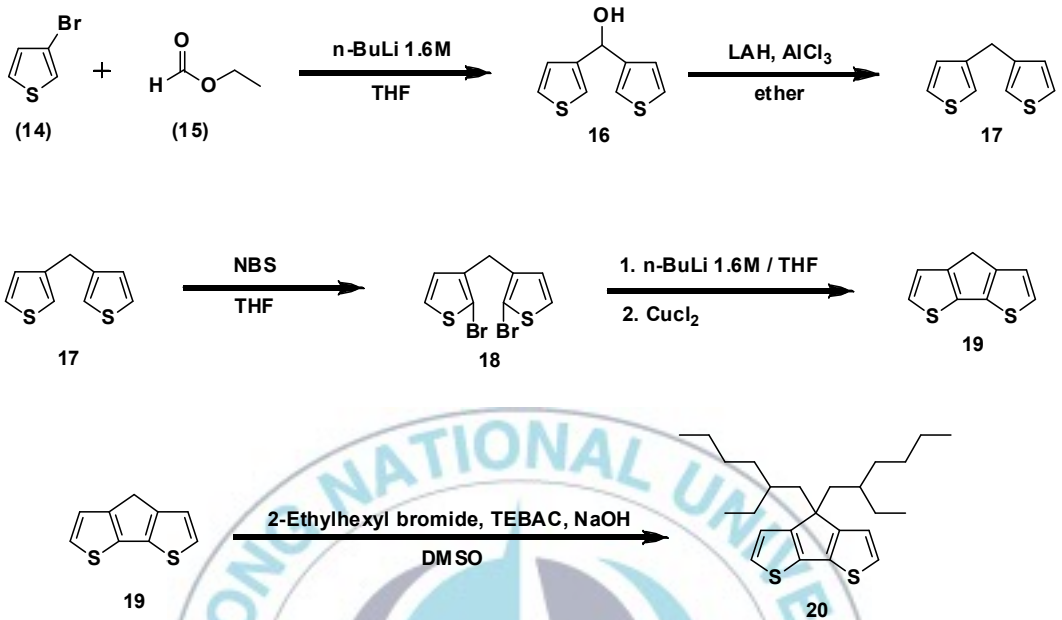

II-1-1-4. Preparation of 2,6-bis(trimethyltin)-4,8-bis(2-octyloxy)benzo[1,2-*b*:3,4-*b*′]dithiophene

The general synthetic routes toward the monomer are outlined in Scheme **4**. In the first step, commercially available thiophene-3-caboxylic acid **(21)** was chlorinated using oxalyl chloride in methylene chloride to generate thiophene-3-carbonyl chloride **(22)**. *N,N*-Diethylthiophene 3-carboxamide **(23)** was prepared from compound **22** and dietylamine with a yield more than 95%. Then, compound **23** was cyclized using *n*-butyllithium in tetrahydrofuran (THF) at 0 ^{o}C to obtain benzo[1,2-*b*:4,5-*b*′]dithiophene-4,8-dione (**24**). Compound **24**, zinc

powder, ethanol, DMF and aqueous sodium hydroxide solution were stirred and refluxed for 2 h under an inert atmosphere, and then bromooctane and a catalytic amount of tetrabutylammonium bromide were added into the mixture then stirred over 6 h until the color changed to orange. The resulting mixture was cooled to room temperature, diluted with water, and extracted with ethylacetate. The crude product was purified on silica gel chromatography using hexane as eluent. Compound **25** in THF was stirred at -78 ^{o}C. The solution was added *n*-BuLi dropwisely at -78 ^{o}C. Warmed to room temperature, Trimethyltin chloride was added at -78 ^{o}C. The mixture was recrystallized using methanol.

Scheme 4. Synthetic route of donor monomer

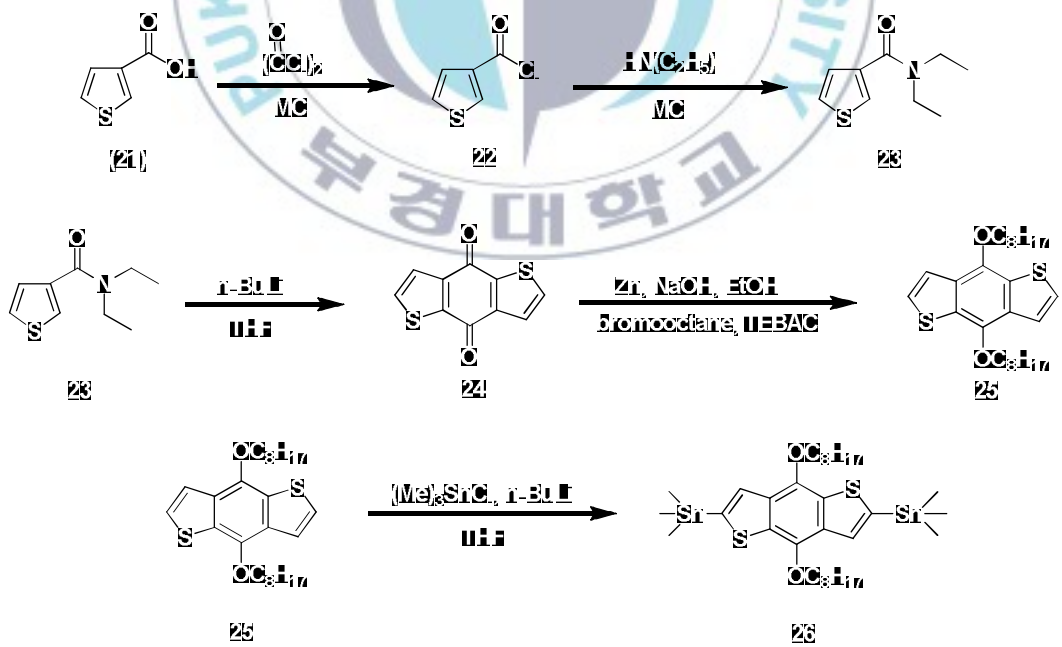

II-1-1-5. Preparation of 4,4-dioctyl-2,6-bis(trimethylstannyl)-4H-silolo[3,2-b:4,5-b']dithiophene

The synthetic route of 4,4-dioctyl-2,6-bis(trimethylstannyl)-4H-silolo[3,2-b:4,5-b']dithiophene is outlined in Scheme 5. To a solution of 2,3-dibromothiophene) in dry ether was added a 1.6 M solution of n-BuLi in hexane dropwise at - 78 ^{o}C. After stirring at -78 ^{o}C for 1h,$CuCl_2$ was introduced to the solution. And n-BuLi in hexane, THF at –78 ^{o}C was added dropwise 3,3'-dibromo-2,2'-bithiophene **(27)** dissolved in THF. Immediately following this addition of dichlorodi-n-octylsilane in THF was added dropwise to obtain 3,3'-Di-n-octylsilylene-2,2'-bithiophene. Compound in THF was n-BuLi in hexane at –78 ^{o}C where a solution of methyltin chloride in THF was added dropwise. The product was further dried by pulling vacuum on a high vac line for 48 hours yielding 3.4 g (95.7 %) of pale green oil.

Scheme 5. Synthetic route of donor monomer

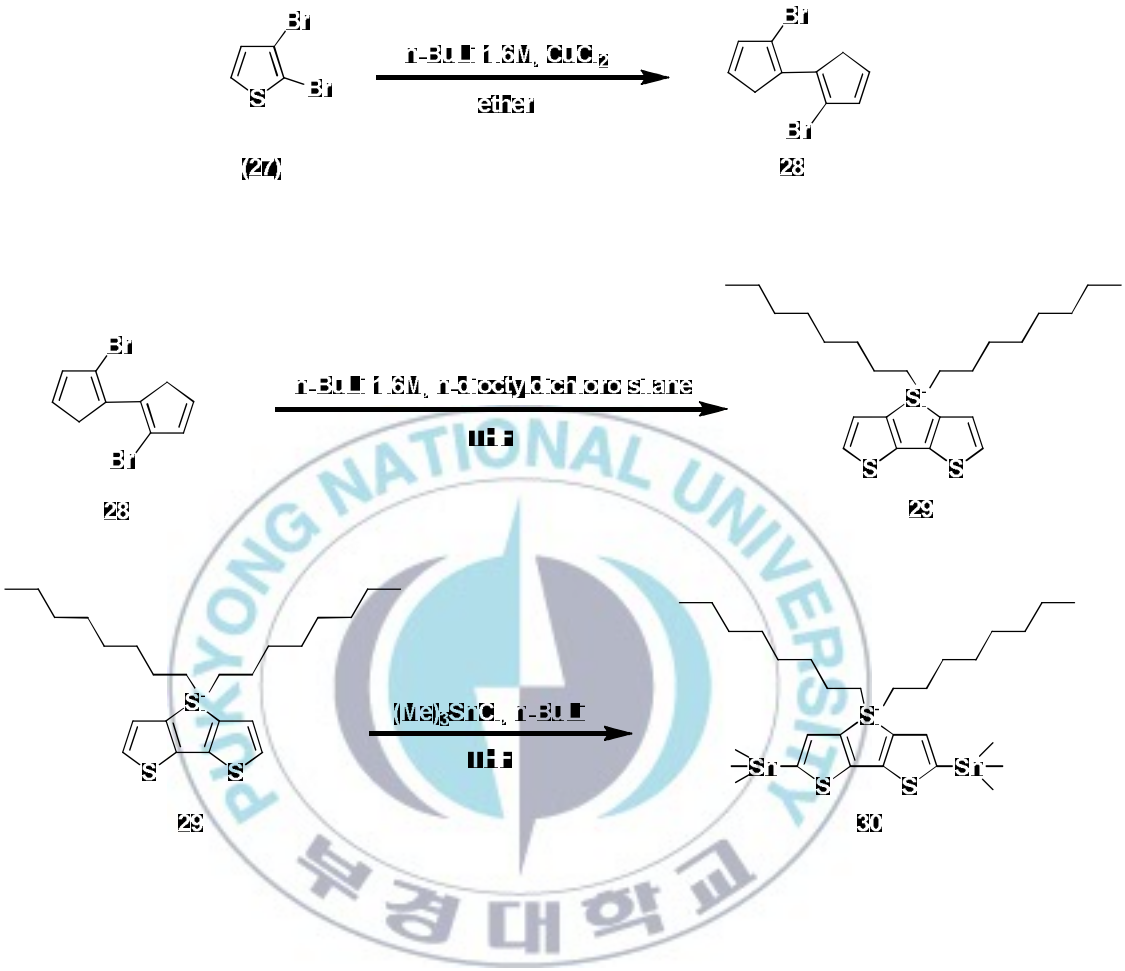

II-1-1-6. Preparation of 2,2'-(9,9-bis(2-ethylhexyl)-9H-fluorene-2,7-diyl)bis(4,4,5,5-tetramethyl-1,3,2-dioxaborolane)

The synthetic route of 2,2'-(9,9-bis(2-ethylhexyl)-9H-fluorene-2,7-diyl)bis(4,4,5,5-tetramethyl-1,3,2-dioxaborolane) is outlined in Scheme **6**. fluorene, iodine and CH_2Cl_2 , bromine diluted with CH_2Cl_2 (20 mL) was added dropwisely at 0 °C. After 12 h, a solution of sodium bisulfite in water was added

and the mixture was stirred for 30 min to become colorless. 2,7-dibromofluorene and tetrabutylammonium bromide in DMSO aqueous sodium hydroxide solution and (2- ethylhexyl)bromide were added to obtain 2,7-Dibromo-9,9'-bis(2-ethylhexyl)fluorine. Compound in anhydrous THF was added n-BuLi at -78°C. before 2-isopropoxy-4,4,5,5-tetramethyl-[1,3,2]dioxaborolane was added in one portion. The residue was recrystallized with acetone to yield 2a (0.680 g, 44%) as a white crystal.

Scheme 6. Synthetic route of donor monomer

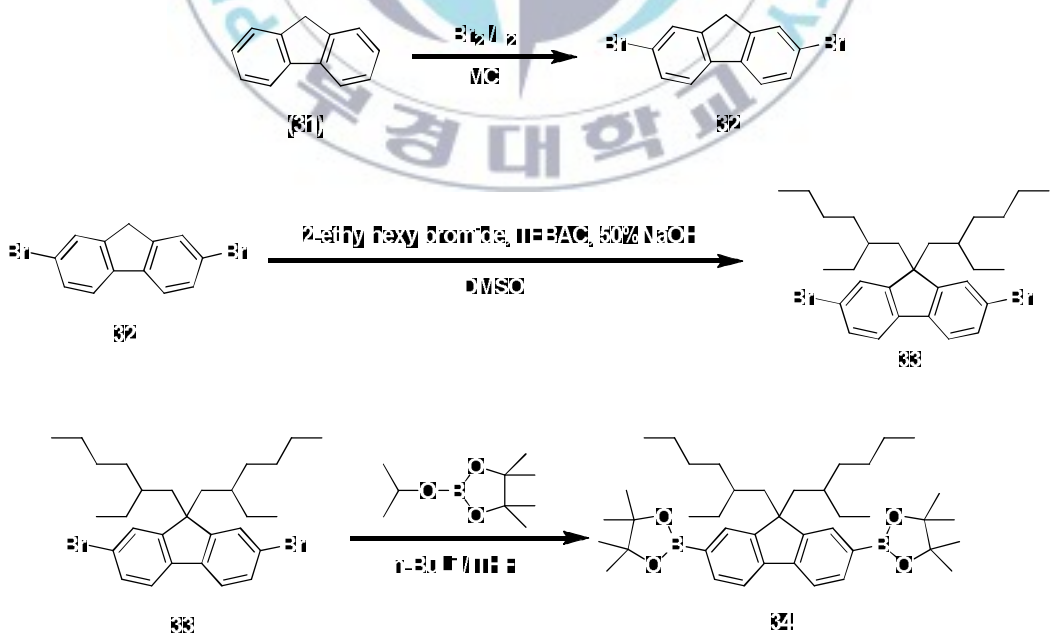

II-1-1-7. Preparation of 9-(heptadecan-9-yl)-2,7-bis(4,4,5,5-tetramethyl-1,3,2-dioxaborolan-2-yl)-9H-carbazole

The synthetic route of 9-(heptadecan-9-yl)-2,7-bis(4,4,5,5-tetramethyl-1,3,2-dioxaborolan-2-yl)-9H-carbazole is outlined in Scheme **7**. HNO_3 and AcOH was added dropwisely 4,4'-Dibromobiphenyl in CH_2Cl_2 and Ac_2O. The reaction was poured into H_2O containing NaOH to partially neutralize the acid, resulting in the formation of a tacky yellow precipitate. 4,4'-Dibromo-2-nitrobiphenyl and triethyl phosphate in CH_2Cl_2 were stirred under nitrogen at 150 °C to obtain **2,7-Dibromocarbazole.** Toluene-4-sulfonic acid heptadec-9-yl ester in DMSO was added dropwise over 1 h to mixture of 2,7- dibromo-9-H-carbazole, freshly powdered KOH and DMSO at room temperature. Upon complete addition the mixture was stirred at room temperature for 6 h then poured into water and the aqueous layer extracted with hexane. Compound in anhydrous THF was added n-BuLi at -78°C. before 2-isopropoxy-4,4,5,5-tetramethyl-[1,3,2]dioxaborolane was added in one portion. The residue was recrystallized with acetone to yield 2a (0.680 g, 44%) as a white crystal.

Scheme 7. Synthetic route of donor monomer

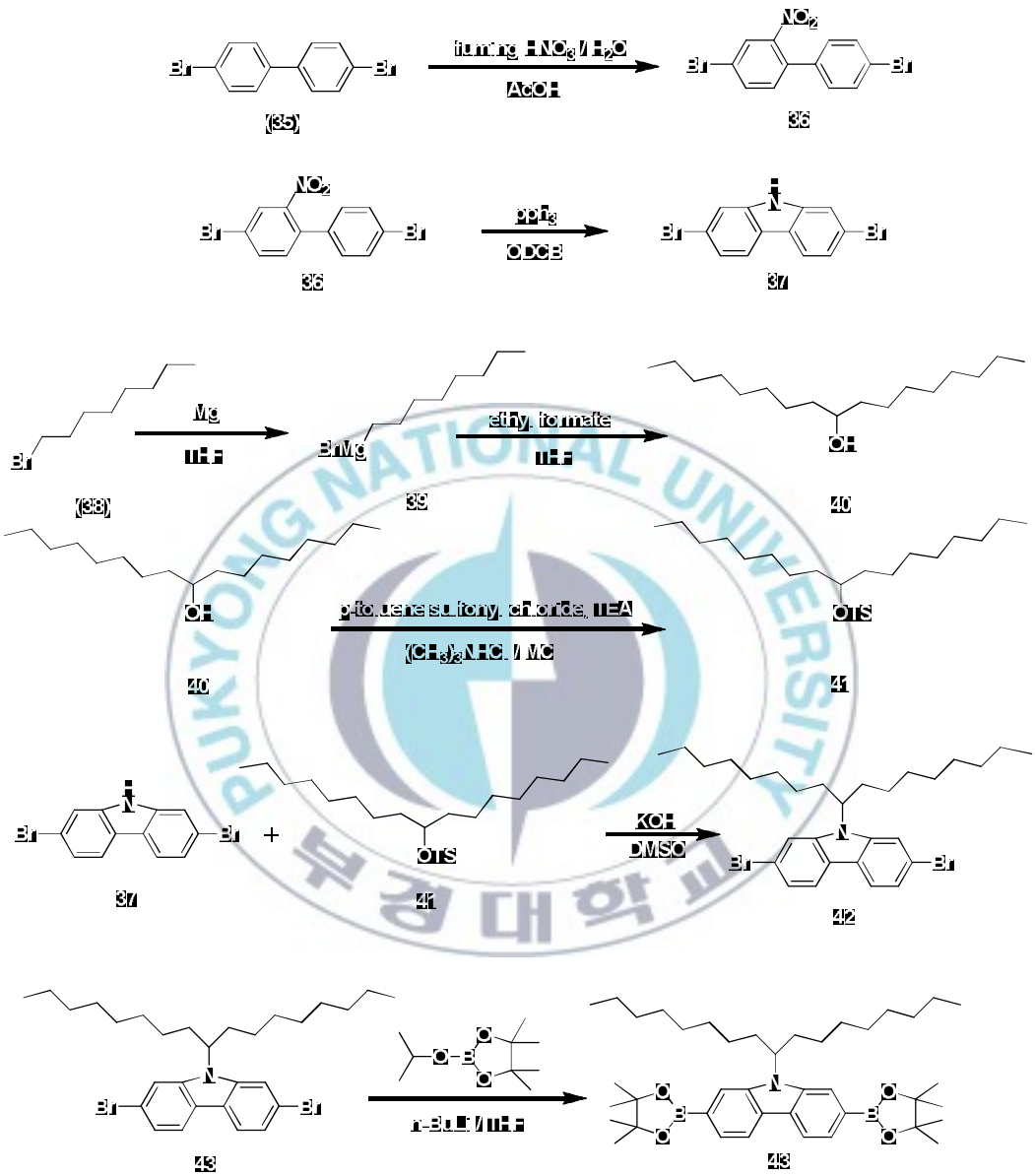

II-1-2. Preparation of polymer

II-1-2-1. Preparation of Poly-(5-(4,8-bis(octyloxy)-6-phenylbenzo[1,2-b:4,5-b']dithiophen-2-yl))-6,7-difluoro-2,3-dihexyl-8-phenylquinoxaline (YJ-6)

Carefully purified Synthesis of 5,8-Dibromo-6,7-difluoro-2,3-dihexylquinoxaline **(9)** as acceptor and 6-Bis(trimethyltin)-4,8-bis(2-octyldodecyloxy)benzo[1,2-*b*:3,4-*b'*]dithiophene **(26)** as donor were polymerized through Stille coupling condition using Tris(dibenzylideneacetone)dipalladium(0) to yield alternating.

Scheme 8. Synthetic route of polymer

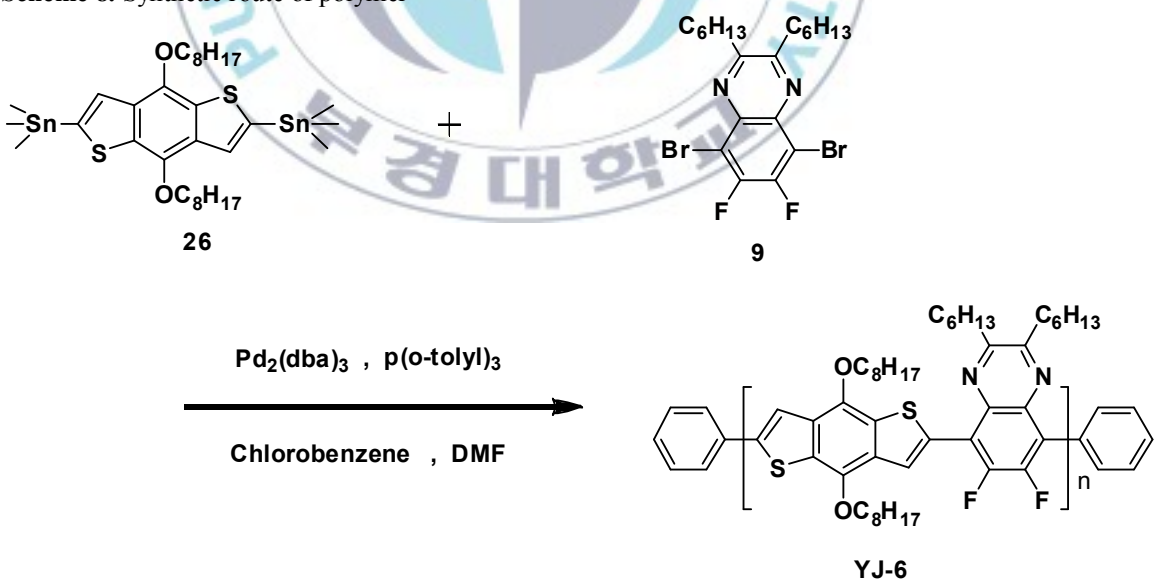

II-1-2-2. Preparation of Poly-(5-(4,4-bis(2-ethylhexyl)-6-methyl-4H-cyclopenta[1,2-b:5,4-b']dithiophen-2-yl))-6,7-difluoro-2,3-dihexyl-8-methylquinoxaline(YJ-7)

Carefully purified Synthesis of 5,8-Dibromo-6,7-difluoro-2,3-dihexylquinoxaline **(9)** as acceptor and 4,4-Di(2-ethtylhexyl)-4H-cyclopenta[2,1-b:3,4-b(]dithiophene **(20)** as donor were polymerized through direct arylation condition using Palladium**(II)** acetate to yield alternating.

Scheme 9. Synthetic route of polymer

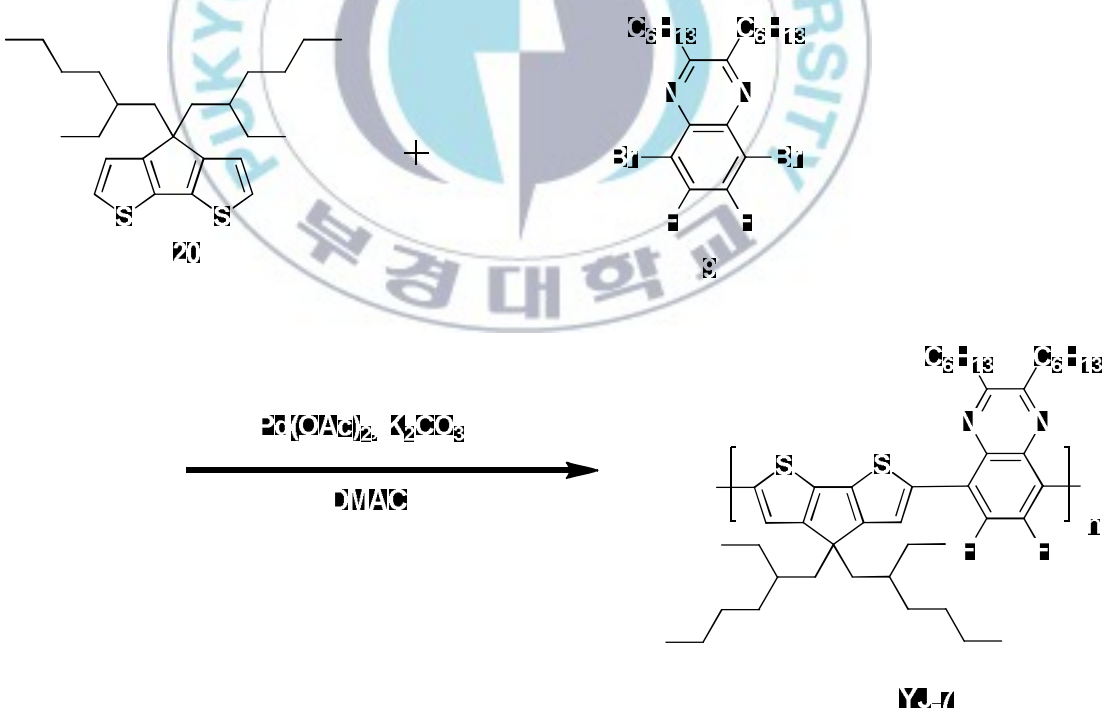

II-1-2-3. Preparation of Poly-(6,7-difluoro-2,3-dihexyl-5-methyl-8-(6-methyl-4,4-dioctyl-4H-silolo[3,2-b:4,5-b']dithiophen-2-yl))quinoxaline (YJ-8)

Carefully purified Synthesis of 5,8-Dibromo-6,7-difluoro-2,3-dihexylquinoxaline **(9)** as acceptor and 5,5'*Bis*(trimethylstannyl)-3,3'-Di-n-dodecylsilylene-2,2'-bithiophene **(30)** as donor were polymerized through Stille coupling condition using Tris(dibenzylideneacetone)dipalladium(0) to yield alternating.

Scheme 10. Synthetic route of polymer

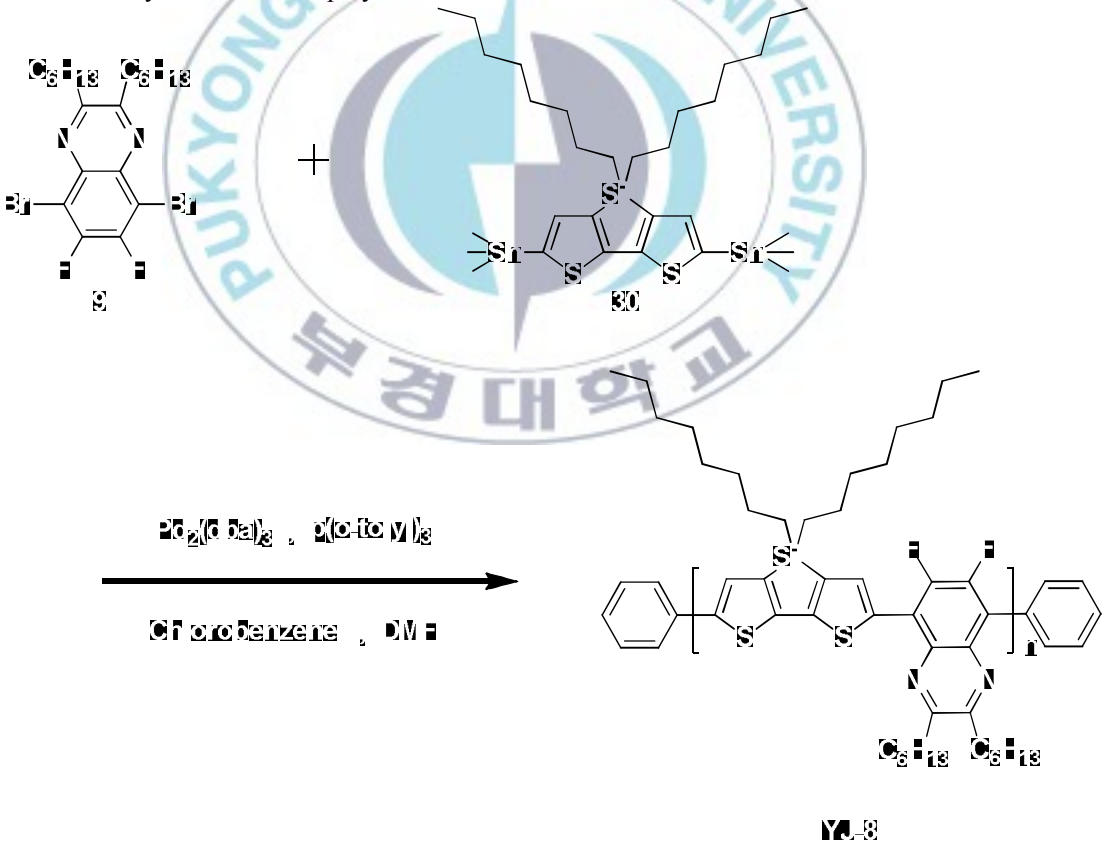

II-1-2-4. Preparation of Poly-(5-(5-(4,8-bis(octyloxy)-6-phenylbenzo[1,2-b:4,5-b']dithiophen-2-yl)thiophen-2-yl))-6,7-difluoro-2,3-dihexyl-8-(5-phenylthiophen-2-yl)quinoxaline (YJ-9)

Carefully purified Synthesis of 5,8-bis(5-bromothiophen-2-yl)-6,7-difluoro-2,3-dihexylquinoxaline**(13)** as acceptor and 6-Bis(trimethyltin)-4,8-bis(2-octyldodecyloxy)benzo[1,2-*b*:3,4-*b*']dithiophene **(26)** as donor were polymerized through Stille coupling condition using Tris(dibenzylideneacetone)dipalladium(0) to yield alternating.

Scheme 11. Synthetic route of polymer

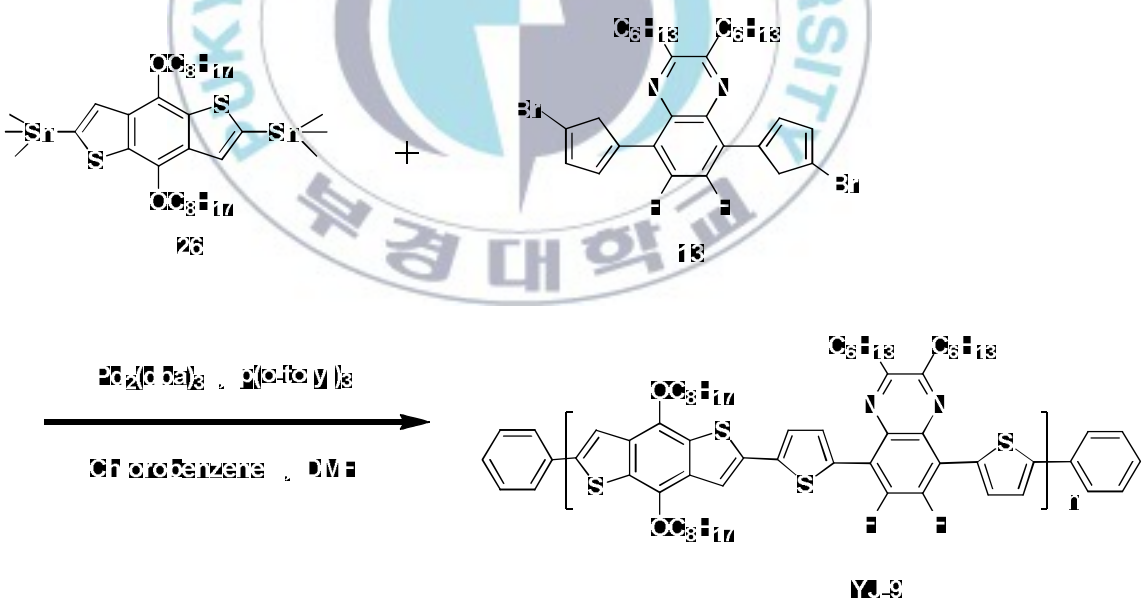

II-1-2-5. Preparation of Poly-(5-(5-(9,9-bis(2-ethylhexyl)-7-phenyl-9H-fluoren-2-yl)thiophen-2-yl))-6,7-difluoro-2,3-dihexyl-8-(5-phenylthiophen-2-yl)quinoxaline (YJ-10)

Carefully purified Synthesis of 5,8-bis(5-bromothiophen-2-yl)-6,7-difluoro-2,3-dihexylquinoxaline**(13)** as acceptor and 2,2'-(9,9-Bis(n-propyl)-fluoren-2,7-diyl)-bis[4,4,5,5-tetramethyl-[1,3,2]dioxaborolane] **(34)** as donor were polymerized through Suzuki coupling condition using Tetrakis(triphenylphosphine) Palladium(0) to yield alternating.

Scheme 12. Synthetic route of polymer

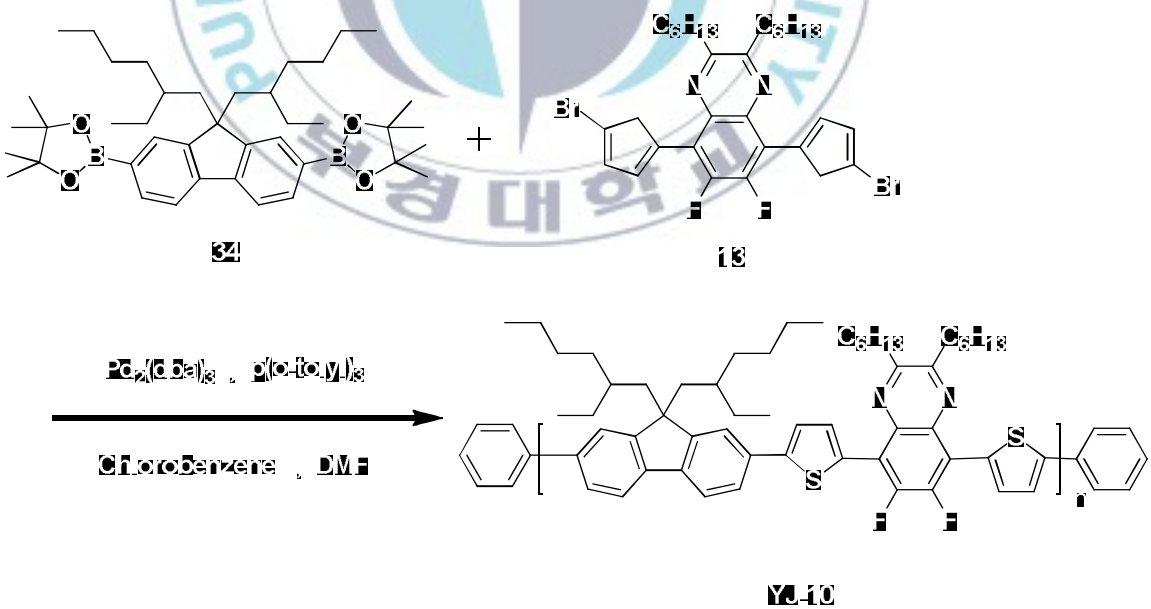

II-1-2-6. Preparation of Poly-(2-(5-(6,7-difluoro-2,3-dihexyl-8-(5-phenylthiophen-2-yl)quinoxalin-5-yl)thiophen-2-yl))-9-(heptadecan-9-yl)-7-phenyl-9H-carbazole (YJ-11)

Carefully purified Synthesis of 5,8-bis(5-bromothiophen-2-yl)-6,7-difluoro-2,3-dihexylquinoxaline**(13)** as acceptor and 2,7-Bis(4',4',5',5'-tetramethyl-1',3',2'-dioxaborolan-2'-yl)-*N*-9''-heptadecanylcarbazole **(43)** as donor were polymerized through Suzuki coupling condition using Tetrakis(triphenylphosphine) Palladium(0) to yield alternating.

Scheme 13. Synthetic route of polymer

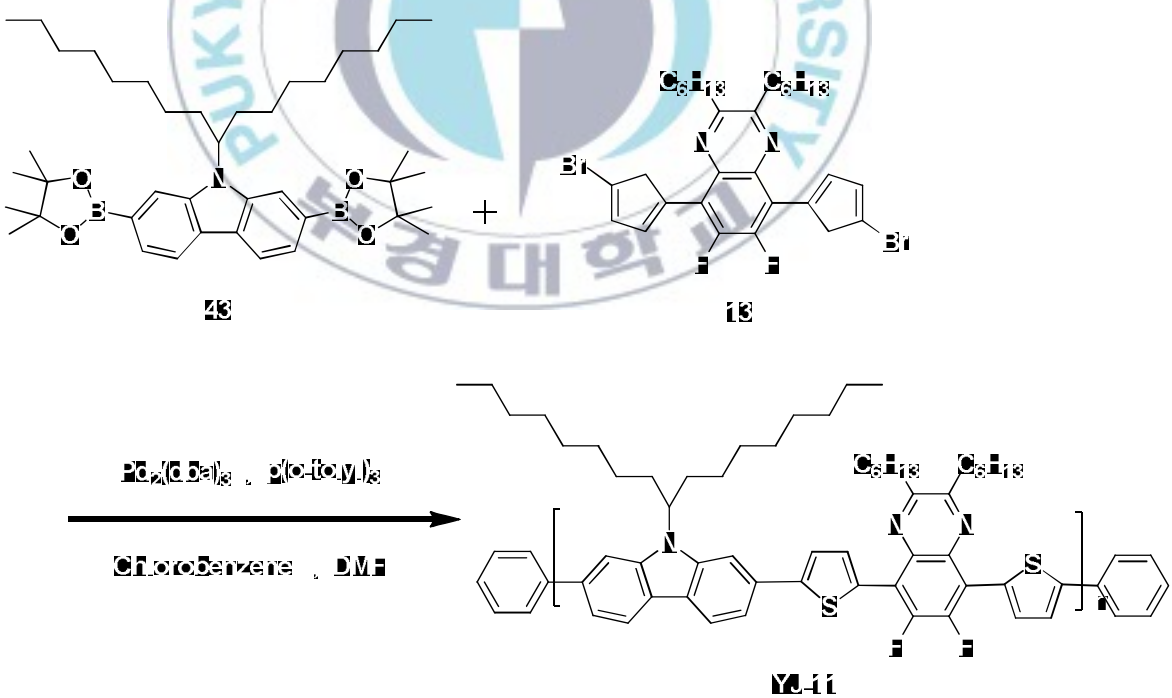

43 13 YJ-11

II-2. Characterization of the Polymers

Table II-1 summarizes the polymerization results including molecular weight, polydispersity index (PDI), and thermal stability of the polymers. The molecular weight (M_n) of 12369 ~ 3063, molecular weight (M_w) of 53055 ~ 3478 with PDI (M_w/M_n) of 4.29 ~ 1.14 of the resulting **YJ-6** ~ **YJ-11** were determined by gel permeation chromatography (GPC). The polymers are easily soluble in common types of organic solvents such as chloroform, tetrahydrofuran (THF), toluene, chlorobenzene and *o*-dichlorobenzene (ODCB).

Table II-1. Polymerization results and thermal properties of polymers

polymer	M_n[a]	M_w[a]	PDI[a]
YJ – 6	9777	15914	1.63
YJ – 7	8257	16145	1.96
YJ – 8	12369	53055	4.29
YJ – 9	3971	7612	1.92
YJ – 10	4015	5226	1.30
YJ – 11	3036	3478	1.14

[a]Number-average molecular weight (M_n), weight-average molecular weight (M_w) and polydispersity of the polymers were determined by gel permeation chromatography (GPC) in Toluene using polystyrene standards.

Figure II-1. Thermogravimetric analysis of polymers

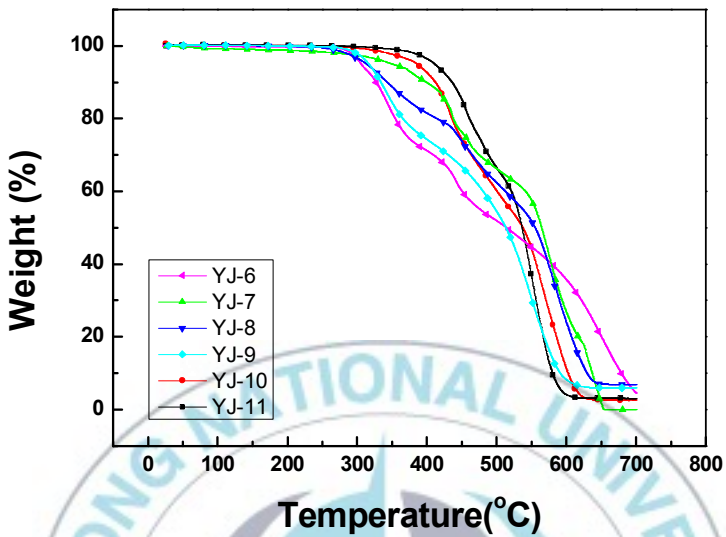

Table II-2. Decomposition temperatures of polymers

polymers	T_d (°C)
YJ - 6	305
YJ – 7	350
YJ – 8	313
YJ – 9	316
YJ – 10	385
YJ - 11	410

Onset decomposition temperatures (T_d) (5% weight loss) measured by TGA under Air

II-3. Optical Properties of the Polymer

Table II-3 summarizes the polymerization results including UV-vis data. The optical properties of the polymer were investigated both in chloroform solution and *o*-dichlorobenzene solution. The absorption spectrum of **YJ-6 ~ 11** exhibited maximum peak at 477 nm ~ 626 nm with solution of chloroform (Figure II-2). Figure II-3 shows the absorption spectra of the polymer in a thin film spin-cast from a solution in chloroform. The significant differences are observed between the solution and the film state. The redshift is observed in the absorption maxima (λmax) relative to dilute solution as a result of a more planar polymer chain structure and/or the degree of interchain π-stacking in the solid film. E_g^{opt}(eV) is the band-gap energy calculated from the intersection of the tangent on the lowest energetic edge of the copolymer thin film absorption spectrum with the baseline by $E_g^{opt}(eV)=1240/\lambda_{edge}$ (nm).

Figure II-2. UV-visible absorption of polymers solution and in chloroform solution (1wt%).

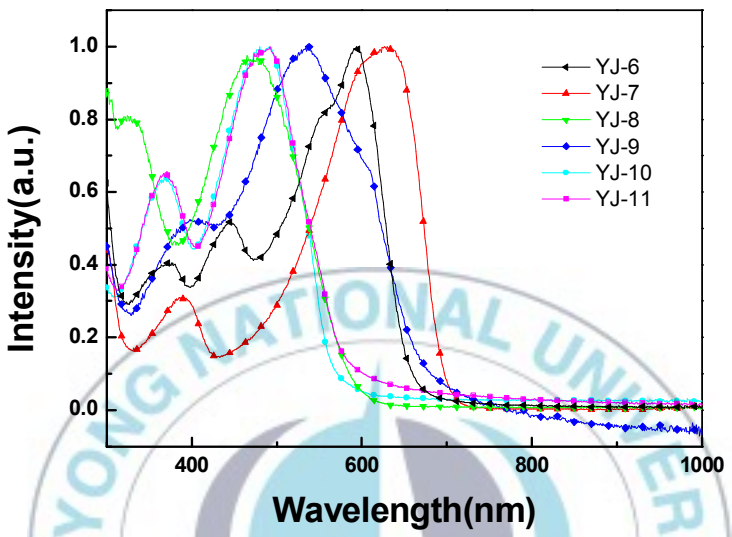

Figure II-3. UV-visible absorption of polymers in a thin film spin-cast from a solution in chloroform (1wt%).

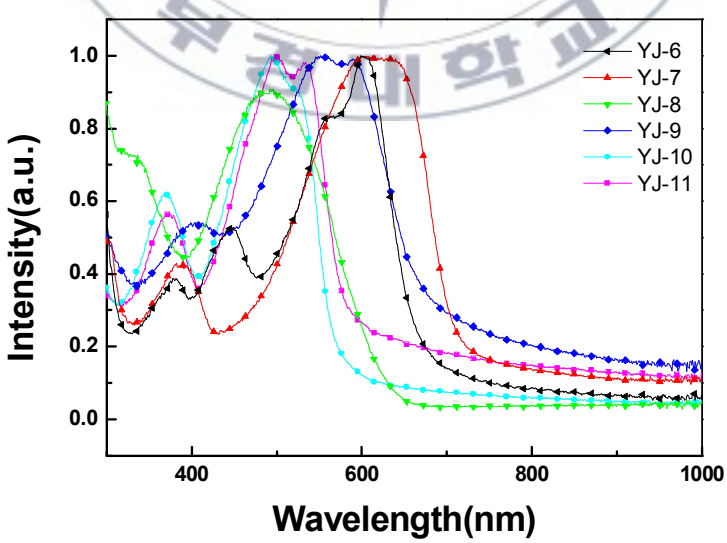

Table II-3. Optical properties of polymer

polymers	Abs.		
	solution	film	
	λ_{max} (nm)	λ_{max} (nm)	λ_{edge} (nm)
YJ-6	593	599	663
YJ-7	626	639	709
YJ-8	477	492	631
YJ-9	538	551	670
YJ-10	479	493	574
YJ-11	491	502	580

In chloroform solution.

II-4. Electrochemical Properties of the Polymer

The electrochemical properties of the polymer were determined from the band gap which were estimated from the absorption edges, and the HOMO energy level which was estimated from the cyclic voltammetry (CV). The CV was performed with a solution of tetrabutylammonium tetrafluoroborate (Bu_4NBF_4; 0.10 M) in acetonitrile at a scan rate of 100 mV/s at room temperature. A platinum electrode (~ 0.05 cm^2) coated with a thin polymer film was used as the working electrode. Pt wire and $Ag/AgNO_3$ electrode were used as the counter electrode and reference electrode, respectively. The energy level of the $Ag/AgNO_3$ reference electrode was determined for 4.80 eV, which was calibrated by the ferrocene /ferrocenium (FC/FC^+) redox system with 4.80 eV. The oxidation potentials is derived from the onset of electrochemical p-doping, and HOMO and lowest unoccupied molecular orbital (LUMO) level was calculated according to the empirical formula, $E_{HOMO} = -([E_{onset}]^{ox} + 4.80)$ eV and $E_{LUMO} = -([E_{onset}]^{red} + 4.80)$ eV, respectively. The polymer exhibits irreversible processes in an oxidation scan.

Figure II-4. Cyclic voltammetry curvres of the polymers in 0.1 M Bu_4NBF_4 acetonitrile solution at a scan rate of 100 mV/s at room temperature (vs an Ag quasi-reference electrode).

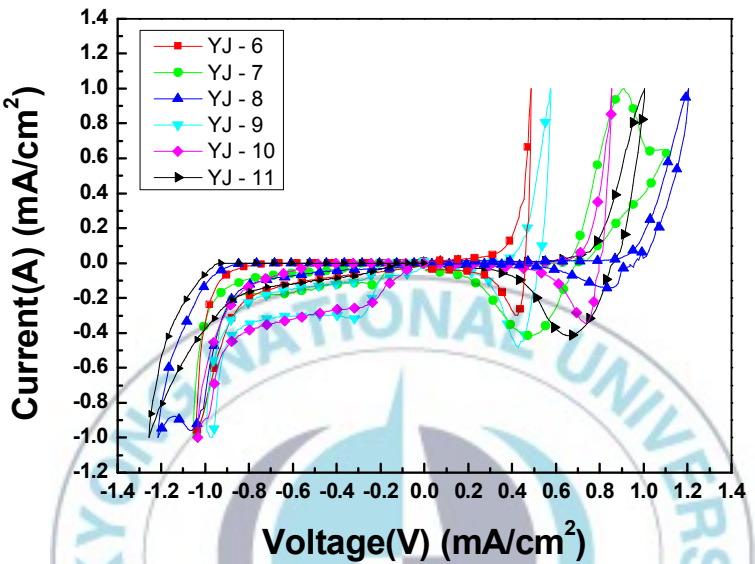

Figure II-5. Energy diagram of HOMO/LOMO levels of small molecule in relation to the work function of the ITO, PEDOT:PSS, PCBM, and Al

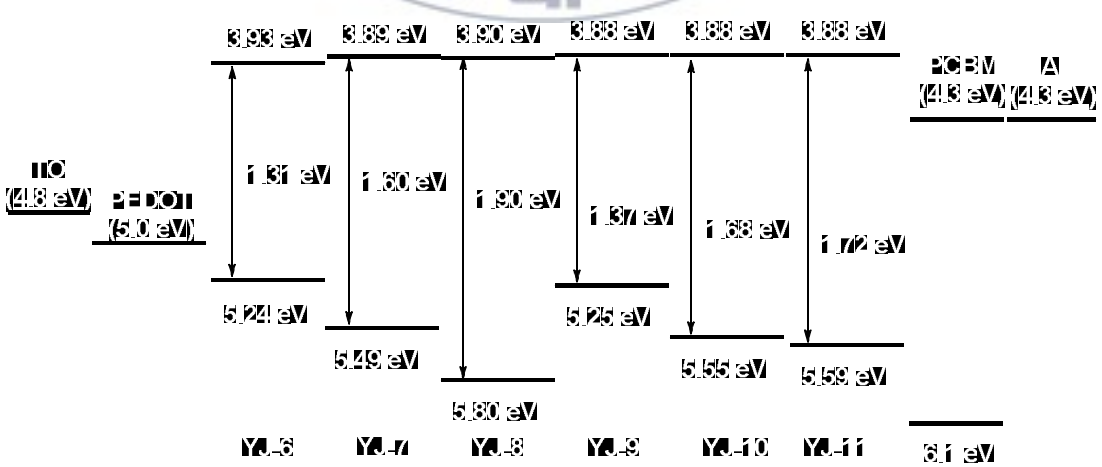

Table II-4. Electrochemical Properties of the Polymers

polymers	optical band gap[a] (eV)	HOMO[b] (eV)	LUMO[c] (eV)	E_{ox}[d] (V)	E_{red}[d] (V)	electrochemical band gap[e] (eV)
YJ-6	1.85	-5.24	-3.93	0.44	-0.87	1.31
YJ-7	1.89	-5.49	-3.89	0.69	-0.91	1.60
YJ-8		-5.80	-3.90	1.00	-0.90	1.90
YJ-9		-5.25	-3.88	0.45	-0.92	1.37
YJ-10		-5.55	-3.88	0.75	-0.92	1.68
YJ-11		-5.59	-3.88	0.79	-0.92	1.72

[a]Optical energy band gap was estimated from the onset wavelength of the optical absorption.. [b]Calculated from the oxidation potentials. [c]Calculated from the reduction potentials. [d]Onset oxidation and reduction potential measuresd by cyclic voltammetry. [e]Calculated from the E_{ox} and E_{red}.

II-5. Photovoltaic Properties of the Polymer

The organic photovoltaic cells, with the sandwiched structure of glass/ITO/PEDOT:PSS/polymer:PCBM/Aluminum, were prepared on commercially available ITO-coated glass substrate (25 × 25 mm^2) with a sheet resistance of ca. 10 Ω/square (Präzisions Glas & Optic GmbH, Germany). Each substrate was patterned using photolithography techniques to produce a segment with an active area of 90 mm^2. Prior to use, the substrates were cleaned with detergent and deionized water. Then, they were ultrasonicated in deionized water and in isopropanol. ITO substrates were spin-coated ((2000 rpm, 60 s) with a thin film (100 nm) of PEDOT: PSS, Baytron P, H. C. Starck) and dried at 120 ℃ for 10 min. A blend of PCBM and polymers (ex. 4.0 mg/mL of polymer in $CHCl_3$) was solubilized overnight in chloroform, filtered through a 0.45 μm poly(tetrafluoroethylene) (PTFE) filter, spin-coated at 2000 rpm for 60 s. The resulting films were dried at 50 ℃ for 10 minutes and then under vacuum at room temperature for 12 hr. The devices were completed by deposition of a 70 nm Al layer. This layer was thermally evaporated at a pressure of 1×10^{-6} Torr at room temperature. Current versus potential curves (*I–V* characteristics) were measured with a Keithley 2400 Digital SourceMeter under a collimated beam. Illumination of the cells was done through the ITO side using light from 150 W Oriel Instruments Solar Simulator and xenon lamp with AM1.5G filter (No. 81094) to

provide an intensity of 90 mW/cm^2.

Current-voltage characteristics of polymers are shown in Figure II-5, II-6. Current density (J_{sc}) of these polymers was in the range of 0.007 ~ 2.65 mA/cm^2, and open circuit voltage (V_{oc}) was 0.25 ~ 0.84 V. The fill factor (FF), and power conversion efficiency were in the range of 0.14 ~ 0.37 and 0.002 ~ 0.776 %, respectively. From the UV-vis absorption data, we expected that PCPDTBCs would show high power conversion efficiencies.

Figure II-6. Current-voltage characteristics for the ITO/PEDOT:PSS/PCPDT-BCs:$PC_{70}BM$(1:3.5)/Al

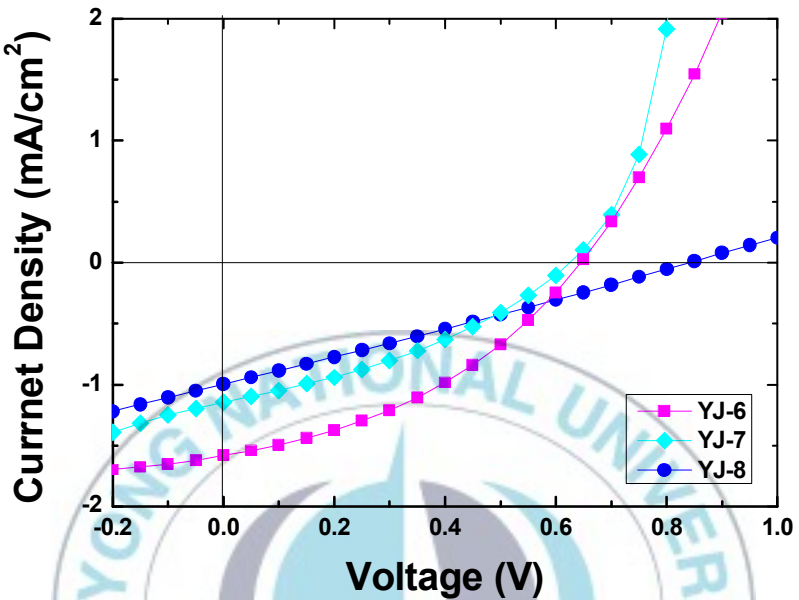

Table II-5. Photovoltaic Properties of PCPDTBCs; open circuit voltage (V_{oc}), short circuit current (J_{sc}), fill factor (FF), power conversion efficiency

	additive	J_{sc} (mA/cm^2)	V_{oc} (V)	FF	PCE (%)
YJ-6 : $PC_{70}BM$	**None**	**1.58**	**0.64**	**0.39**	**0.394**
YJ-7 : $PC_{70}BM$	**DIO(3wt%)**	**1.14**	**0.62**	**0.34**	**0.252**
YJ-8 : $PC_{70}BM$	**None**	**0.99**	**0.84**	**0.26**	**0.219**

Figure II-6. Current-voltage characteristics for the ITO/PEDOT:PSS/PCPDT-BCs:$PC_{60}BM$(1:3.5)/Al

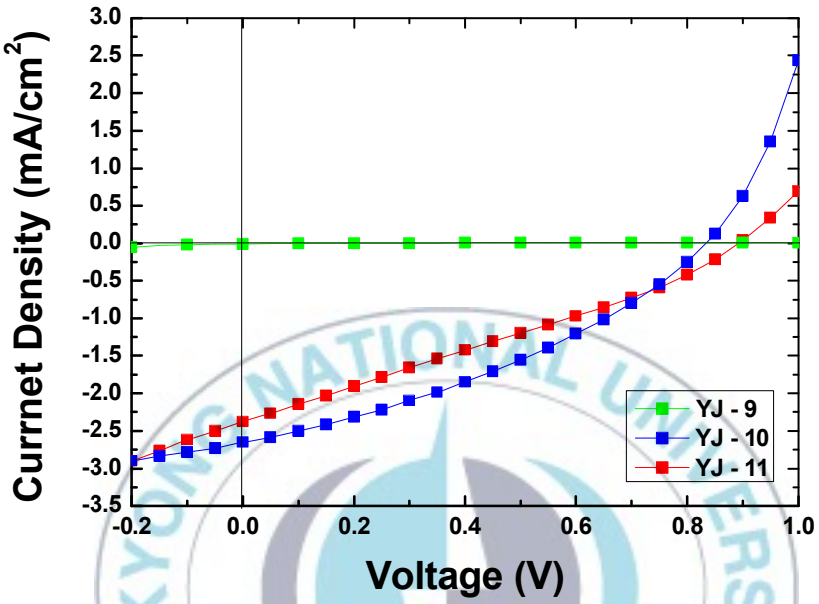

Table II-5. Photovoltaic Properties of PCPDTBCs; open circuit voltage (V_{oc}), short circuit current (J_{sc}), fill factor (FF), power conversion efficiency

	additive	J_{sc} (mA/cm^2)	V_{oc} (V)	FF	PCE (%)
YJ-9 : $PC_{70}BM$	**None**	**0.007**	**0.25**	**0.14**	**0.002**
YJ-10 : $PC_{70}BM$	**None**	**2.65**	**0.84**	**0.35**	**0.776**
YJ-11 : $PC_{70}BM$	**None**	**2.41**	**0.80**	**0.37**	**0.701**

Chapter III. Conclusion

In conclusion, We synthesized acceptor (DFDHQx) and conjugated polymers (YJ-6~YJ-11) using an electron-deficient DFDHQx unit and five different electron-rich aromatic units have been synthesized via a Direct arylation, Stille, Suzuki polymerization reaction. OPVs based on these polymers give high $V_{oc.}$ The best device was based on a YJ-10:$PC_{60}BM$ blend and gave J_{sc} = 2.65 mA/ cm^2, FF = 0.35, and V_{oc} = 0.84 V, resulting in a maximum power conversion efficiency of over 0.776% at an optical band gap of Eg = 1.68 eV.

Chapter IV. Experimental

Materials and Instruments

All reagents were purchased from Aldrich or TCI, and used without further purification. Solvents were purified by normal procedure and handled under moisture-free atmosphere. ^{1}H and ^{13}C NMR spectra were recorded with a Varian Gemini-300 (300 MHz) spectrometer and chemical shifts were recorded in ppm units with TMS as the internal standard. Flash column chromatography was performed with Merck silica gel 60 (particle size 230-400 mesh ASTM) with ethyl acetate / hexane or methanol / methylene chloride gradients unless otherwise indicated. Analytical thin layer chromatography (TLC) was conducted using Merck 0.25 mm silica gel 60F pre-coated aluminum plates with fluorescent indicator UV254. High resolution mass spectra (HRMS) were recorded on a JEOL JMS-700 mass spectrometer under electron impact (EI) or fast atom bombardment (FAB) conditions in the Korea Basic Science Institute (Daegu, Korea). Elemental analyses (EA) were performed by Flash EA 1112 Series. The UV-vis absorption spectra were recorded by a Varian 5E UV/VIS/NIR spectrophotometer. The CV was performed with a solution of tetrabutylammonium perchlorate (Bu_4NClO_4; 0.10 M) in dichloromethane at a scan rate of 100 mV/s at room temperature. Pt wire and $Ag/AgNO_3$ electrode

were used as the counter electrode and reference electrode, respectively. The energy level of the $Ag/AgNO_3$ reference electrode (calibrated by the FC/FC^+ redox system) was 4.40 eV below the vacuum level. HOMO levels were calculated according to the empirical formula (E_{HOMO}= -($[E_{onset}]_{ox}$ + 4.40) eV). For the EL experiment, poly(3,4-ethylenedioxythiophene) (PEDOT) doped with poly(styrenesulfonate) (PSS), as the hole-injection-transport layer, was introduced between emissive layer and ITO glass substrate cleaned by successive ultrasonic treatments. The solution of the PEDOT:PSS in aqueous isopropyl alcohol was spin-coated on the surface-treated ITO substrate and dried on a hot plate for 30 min at 110 °C. On top of the PEDOT:PSS layer, the emissive small molecule film was obtained by spin casting chlorobenzene solution of the small molecule. The emissive small molecule thin film prepared had a uniform surface with a thickness of around 110 nm. The emissive film was dried in vacuum, and aluminum electrodes were deposited on the top of the small molecule films through a mask by vacuum evaporation at pressures below 10^{-7} Torr, yielding active areas of 4 mm^2.

IV-1. Synthesis of acceptor monomer

IV-1-1. Synthesis of 2,3-Difluoro-1,4-bis-(trimethylsilyl)benzene (2).

n-butyllithium (1.6 M in n-hexane, 120 mL, 192 mmol) was added to a solution of di-isopropylamine (27 mL, 192 mmol) in anhydrous THF (80 mL) at -78 ℃. After stirring 30 min at -78 ℃, 1,2-difluorobenzene (7.5 mL, 77 mmol) and chlorotrimethylsilane (24 mL, 192 mmol) were added to the solution at a rate which allowed the internal reaction temperature to remain below -50 ℃. The solution was stirred at -78 ℃ for an additional 1 h. 1 M H_2SO_4 solution (20 mL) was added and then extracted with diethyl ether (20 mL × 3). The combined organic layers were washed with brine, dried over $MgSO_4$, and concentrated under reduced pressure to afford colorless needle-shaped crystals of compound **21** (19.0 g, 98%). ^{1}H NMR ($CDCl_3$): δ 7.09 (s, 2H), 0.32 (s, 18H). LRMS (EI): m/z = 258 (M^+).

IV-1-2. Synthesis of 1,4-dibromo2,3-Difluoro-benzene (3).

To a neat bromine (5.3 mL, 103 mmol) cooled to 0 ℃ was added portion wise solid **21** (8.9 g, 34.4 mmol) while maintaining the internal temperature between 20 and 40 ℃. The reaction mixture was stirred at 58 ℃ for 2 h. After 1 h of this period had elapsed, additional bromine (0.9 mL, 17.2 mmol) was added. The

reaction mixture was cooled to 0 ℃ and slowly poured into ice-cold saturated $NaHCO_3$ solution and extracted with diethyl ether (50 mL × 3). The combined organic layers were washed with brine, dried over $MgSO_4$, and concentrated under reduced pressure to afford colorless liquid of compound **22** (9.2 g, 99%). ^1H NMR ($CDCl_3$): δ 7.23 (m, 2H). LRMS (EI): m/z = 272 (M^+).

IV-1-3. Synthesis of 1,4-dibromo-2,3-difiuoro-5,6-dinitro-benzene (4).

In a 500 mL flask, concentrated sulphuric acid (44 mL) was added and cooled to 0-5°C in an ice water bath. Fuming nitric acid (44 mL) and 2,3-difluoro-1,4-dibromo-benzene (8.8 g, 32.5 mmol) were slowly added. Then, the flask was heated to 65°C for 14 h. The mixture was then precipitated into ice water. The resulting yellow solid was filtered and purified by column with petroleum hexane/CH_2Cl_2 (4:1) to afford a white solid of compound **23** (3.4 g, 29%).

IV-1-4. Synthesis of 3,6-dibromo-4,5-difluorobenzene-1,2-diamine (5).

To a solution of compound **4** (6.3 g, 17.5 mmol) in ethanol (100 mL) and conc. HCl (60mL) was added to $SnCl_2$•$2H_2O$ (39.5 g, 175 mmol) in several portions. The mixture was refluxed for 1 hour and stirred overnight at room temperature. Then, pH value of the mixture was adjusted to 8~9 by adding aqueous KOH solution, and then the mixture was extracted with ethyl acetate three times. The

combined organic phases were dried over anhydrous $MgSO_4$. Further purification was run by silica column with petroleum hexane/CH_2Cl_2 (1:1) to give an white solid of compound **5** (4.6 g, 88%). ^{1}H NMR ($CDCl_3$, ppm): 3.85 (s, 4H). ^{13}C NMR ($CDCl_3$, ppm): 142.99 (d, J = 18.11 Hz), 141.06 (d, J = 17.65 Hz), 129.78, 98.39 (t). ^{19}F NMR ($CDCl_3$, ppm): -139.02. GC-MS (M+, $C_6H_4Br_2F_2N_2$), cacld, 301.9; found: 302.

IV-1-5. Synthesis of Tetradecane-7,8-dione (6).

A Grignard reagent was prepared by the dropwise addition of the respective hexyl bromide (152 mmol) to a stirred suspension of iodine-activated magnesium[6] (4.0 g, 165 mmol) in THF (100 mL). In a separate flask, LiBr (25.5 g, 293 mmol) in THF (110 mL) was added to a stirred suspension of CuBr (21.1 g, 146 mmol) in THF (110 mL) to form a pale green suspension. This mixture was then cooled to -100 °C via a pentane/liquid nitrogen bath. The Grignard reagent was slowly added to the LiBr/CuBr suspension by cannula such that the temperature of the reaction mixture did not exceed -75°C. Oxalyl chloride (7.77 g, 61.0 mmol) was then added slowly via syringe to maintain a temperature below -70°C. The mixture was stirred at -90 to -95°C for 60 min, allowed to warm to room temperature and quenched with saturated aqueous NH_4Cl. The organic layer was separated and the aqueous layer extracted repeatedly with ethyl acetate. The combined organic layers were dried with anhydrous $MgSO_4$, concentrated by

rotary evaporation, and separated on a silica column using a petroleum ether/ethyl acetate (95:5) to give a yellow solid of compound **6** (10.91g, 76%). ^{1}H NMR δ 0.86 (t, J = 7.2 Hz, 6H), 1.24 (m, 12H), 1.56 (p, J = 7.2 Hz, 4H), 2.72 (t, J = 7.2 Hz, 4H), ^{13}C NMR δ 14.2, 22.7, 23.2, 29.0, 31.7, 36.3, 200.4.

IV-1-6. Synthesis of 5,8-Dibromo-6,7-difluoro-2,3-dihexylquinoxaline (9).

The compound **6** (4.2 g, 14.0 mmol) and Tetradecane-7,8-dione (3.81 g, 16.9 mmol) were dissolved in ethanol (15 mL) and acetic acid (15 mL). The mixture was refluxed overnight. After cooling to room temperature, the resultant mixture was poured into water and extracted with ethylacetate. After dried over $MgSO_4$ and purified by silica column with petroleum hexane/CH_2Cl_2 (10:1) to give an yellow solid of compound **9** (1.3 g, 18%). ^{1}H NMR (600 MHz, $CDCl_3$): δ (ppm) = 7.92 (s, 2H), 7.66 (d, 4H), 7.40-7.42 (t, 2H), 7.35 (t, 4H), ^{13}C NMR (125 MHz, $CDCl_3$): δ (ppm) = 154.1, 139.3, 138.0, 133.1, 130.3, 129.6, 128.4, 123.7. FT-IR (KBr, ν/cm^{-1}) = 3061, 1584, 1496, 1454, 1384, 1332, 1304, 1176, 1060, 1026, 988, 897, 828, 773, 656, 578, 536.

IV-2. Synthesis of acceptor monomer

IV-2-1. Synthesis of 6,7-difluoro-2,3-dihexyl-5,8-di(thiophen-2-yl) quinoxaline (12)

5,8-Dibromo-6,7-difluoro-2,3-dihexylquinoxaline **(9)** (5.63 g, 11.44 mmol), 2-(tributylstanny)thiophene **(11)** (17.08 g, 6.42 mmol), and $Pd(PPh_2)Cl_2$ were charged in a 250 mL round-bottomed flask, followed by addition of 75 mL of THF. The mixture was heated to 110 °C and maintained for 24 h. After cooling, the product was obtained yellow crystal by column chromatography (silica gel, dichloromethane/ hexane) 1 : 20) yielded **12** (5.43g, 10.71 mmol, 93.6%) ^{1}H NMR ($CDCl_3$) δ 7.10 (m, 9H), δ 7.24 (m, 6H), δ 7.46 (m, 2H); ^{13}C NMR (75 MHz, $CDCl_3$) δ 122.33, 123.13, 123.88, 124.10, 124.53, 124.53, 126.83, 128.08, 128.64, 129.41, 144.34, 147.28, 147.5

IV-2-2. Synthesis of 5,8-bis(5-bromothiophen-2-yl)-6,7-difluoro-2,3-dihexylquinoxaline (13)

NBS (3.88 g, 21.78 mmol) was slowly added to an ice-cooled and stirred solution of **12** (5.34 g, 10.71 mmol) in THF (80 mL). The mixture was allowed to reach room temperature overnight and then extracted with diluted hydrochloric acid and diethyl ether. The diethyl ether layer was washed with water and brine. The organic solvent layers were evaporated under reduced pressure and column

chromatography (silica, eluent heptane) yielded **13** (5.38 g, 8.20 mmol, 75.25%) of a green solid. 1H-NMR: 7.18 (d, J¼5.2 Hz, 2H), 6.73 (d, J¼6.0 Hz, 2H), 3.86 (s, 2H). 13C-NMR: 138.79 (q), 128.46 (t), 125.70 (t), 109.80 (q), 29.47 (s).

IV-3. Synthesis of donor monomer

IV-3-1. Synthesis of Di-3-thienylmethanol (16)

n-BuLi in hexanes (69.27 mL,1.6 M) was slowly added to a solution of **14** (10 mL, 105.56 mmol) in dry diethyl ether (25 mL) at -78 °C. The mixture was stirred for 30 min at -78 °C. Then **15** (3.91 mL, 48.57 mmol) was added dropwise. This mixture was allowed to reach room temperature overnight. The reaction mixture was washed with acid, base, and brine. The organic layer was dried on sodium sulfate and the solvent was evaporated under reduced pressure. The crude product, which was 10.51g (50.72%) pure, was taken to the next reaction without further purification

IV-3-2. Synthesis of Di-3-thienylmethane (17)

AlCl3 (8.35 g, 59.91 mmol) was added to a solution of $LiAlH_4$ (1.895 g, 49.93 mmol) in dry diethyl ether (120 mL) at room temperature. To this mixture crude

16 (9.8 g) was added dropwise. This mixture was refluxed for 3 h after which the reaction mixture was washed with hydrochloric acid (150 mL), NaOH solution (150 mL), and twice with brine (150 mL). All water layers were once extracted with diethyl ether. The combined organic layers were dried on sodium sulfate and subjected to column chromatography (silica, hexane). This resulted in 6.75g (75.01%) of **17** as a colorless oil. 1H-NMR: 7.26 (dd, J¼3.6 Hz, 2H), 6.95 (dd, J¼4.2Hz, 2H), 6.94 (t, J¼4.8 Hz, 2H), 3.99 (s, 2H). 13CNMR: 140.99 (q), 128.40 (t), 125.61 (t), 121.17 (t), 31.11 (s).

IV-3-3. Synthesis of Bis(2-bromothien-3-yl)methane (18)

NBS (18.766 g, 105.85 mmol) was slowly added to an ice-cooled and stirred solution of **17** (9.5 g, 52.93 mmol) in THF (280 mL). The mixture was allowed to reach room temperature overnight and then extracted with diluted hydrochloric acid and diethyl ether. The diethyl ether layer was washed with water and brine. The organic solvent layers were evaporated under reduced pressure and column chromatography yielded **18** (13.67 g, 76.39%) of a colorless oil. 1H-NMR: 7.18 (d, J¼5.2 Hz, 2H), 6.73 (d, J¼6.0 Hz, 2H), 3.86 (s, 2H). 13C-NMR: 138.79 (q), 128.46 (t), 125.70 (t), 109.80 (q), 29.47 (s).

IV-3-4. Synthesis of 4H-Cyclopenta[2,1-b:3,4-b(]dithiophene (19)

18 (14 g, 41.41 mmol) was added to activated copper (II)chloride (5.57 g, 41.41 mmol) in dry THF (270 mL). This mixture was stirred at an internal temperature of 145 ℃ for 3 h. The reaction mixture was repeatedly extracted with water and heptane and the organic layers were combined. The solids that resulted after evaporation of the organic solvent were recrystallized from methanol to yield **19** (2.37 g, 32.1%) as offwhite flakes. 1H-NMR: 7.18 (d, J¼5.2 Hz, 2H), 7.09 (d, J¼4.8 Hz, 2H), 3.54 (s, 2H). 13C-NMR: 149.65 (q), 138.64 (q), 124.45 (t), 122.94 (t), 31.81 (s).

IV-3-5. Synthesis of 4,4-Di(2-ethtylhexyl)-4H-cyclopenta[2,1-b:3,4-b(]dithiophene (20)

To a solution of **19**(2.2 g, 12.34 mmol) in DMSO, powdered NaOH (1.15 g, 30.85mmol) followed by 2- ethylhexylbromide (4.33 g, 30.85 mmol). This mixture was stirred at room temperature overnight and then poured out in water and heptane. The organic layer was washed two times with water and one time with brine. The heptane was evaporated in vacuo and the resulting light yellow oil was subjected to column chromatography (silica, eluent heptane) to yield **20** as a light-yellow oil (3.1 g, 62.38%). 1H-NMR: 7.10 (d, J¼4.4 Hz, 2H), 6.91 (m, 2H),

1.85 (m, 2H), 0.90 (m, 18H), 0.75 (t, 2H), 0.58 (t, 2H). 13CNMR: 157.59 (q), 136.77 (q), 123.92 (t), 122.30 (t), 53.22 (q), 43.21 (s), 34.97 (s), 34.11 (s), 28.57 (s), 27.24 (s), 22.74 (s), 14.07 (p), 10.63 (p).

IV-4. Synthesis of donor monomer

IV-4-1. Synthesis of thiophene-3-carbonyl chloride (22)

Thiophene-3-carboxylic acid (10 g, 78.03 mol) and 100 mL of methylene chloride were put into a 250 mL flask. The mixture was cooled by ice-water bath, and then oxalyl chloride (78.03 g, 156.07 mol) was added in one portion. The reactant was stirred overnight at ambient temperature, and a clear solution was obtained. After removing the solvent and unreacted oxalyl chloride by rotary evaporation, compound **22** was obtained as colorless solid. It was dissolved into 100 mL of methylene chloride and used for the next step.

IV-4-2. Synthesis of *N,N*-diethylthiophene-3-carboxamide (23)

In a 250 mL flask in ice-water bath, 16.15 mL of diethylamine (156.07 mol) and 100 mL of methylene chloride were mixed, and the solution of thiophene-3-carbonyl chloride was added into the flask slowly. After all of the solution was

added, the ice bath was removed, and the reactant was stirred at ambient temperature for 30 min. Then, the reactant was washed by water several times, and the organic layer was dried over anhydrous $MgSO_4$. After removing solvent, the crude product was purified by flash chromatography (60 × 120 mm column, SiO_2, EtOAc/hexane, 1:4) to give 12 g (91%) of compound **23** as pale yellow oil ; ^{1}H NMR (300 MHz, CDCl3): δ 7.46 (d, 1H, *J* = 1.09 Hz), 7.30 (t, 1H, *J* = 1.09 and 4.94 Hz), 7.17 (d, 1H, *J* = 4.94 Hz), 1.18 (m, 10H) ; ^{13}C NMR (75 MHz, $CDCl_3$) δ 166.64, 137.53, 13.08, 125.88, 43.32, 14.59, 39.81 HRMS(EI^+, m/z) $[M]^+$ calcd for $C_9H_{13}NOS$ 183.0718 measured 183.0717

IV-4-3. Synthesis of 4,8-dihydrobenzo[1,2-*b*:4,5-*b′*]dithiophen-4,8-dione (24)

Compound **23** (70.93 mol, 12 g) was put into a well-dried flask with 25 mL of THF under an inert atmosphere. The solution was cooled down by an ice-water bath, and 32 mL of *n*-butyllithium (85.12 mol, 2.5 mol/L) was added into the flask dropwise within 30 min. Then, the reactant was stirred at ambient temperature for 2 hrs. The reactant was poured into ice water and stirred for several hours. The mixture was filtrated, and the yellow precipitate was washed by 100 mL of water, 50 mL of methanol, and 50 mL of hexane successively. 7.5 g of compound **3** was obtained as a yellow powder (34.04 mmol, yield 96%). Mp 241 ^{o}C ; ^{1}H NMR (300 MHz, CDCl3): δ 7.15 (d, 2H, *J* = 4.94 Hz), 6.46 (d, 2H, *J*

= 5.22 Hz) ; ^{13}C NMR (75 MHz, $CDCl_3$) δ 174.69, 145.14, 143.06, 133.78, 126.81 HRMS(EI^+, m/z) $[M]^+$ calcd for $C_{10}H_4O_2S_2$ 219.9653 measured 219.9652

IV-4-4. Synthesis of 4,8-Bis(2-octyloxy)benzo[1,2-*b*:3,4-*b*]dithiophene (25)

To a mixture of 4,8-dihydrobenzo[1,2-*b*:4,5-*b*']dithiophen-4,8-dion (4 g, 18 mmol) and zinc powder (2.6 g, 40 mmol) was added 5N NaOH aqueous solution (37 mL) and the mixture was stirred under reflux for 3 h, After bromooctane(22.26 g, 54 mmol) and tetrabutylammoniumbromide (0.9 g, 3.64 mmol) were added to the mixture, the reaction mixture was further refluxed for 12 h. The reaction mixture was then extracted with diethyl ether, and the organic layer was washed with brine and dried over anhydrous NaSO4. After evaporating the solvent, the crude product was purified by silica gel chromatography using hexane to yield as a colorless sticky oil (4.9 g, 6.25 mmol, 35%). ^1H NMR (300 MHz, CDCl3): δ 7.47 (d, 2H, J= 5.76 Hz), 7.36 (d, 2H, J = 5.76 Hz), 4.17 (d, 4H, J = 5.49 Hz), 1.88-1.82 (m, 2H), 1.67-1.60 (m, 4H), 1.53-1.20 (m, 60H), 0.90-0.87 (m, 12H) ; ^{13}C NMR (75 MHz, CDCl3): δ 144.88, 131.72, 130.161, 126.10, 120.49, 39.44, 32.17, 31.56, 30.31, 29.94, 29.91, 29.88, 29.61, 27.23, 22.94, 14.37 HRMS(FAB^+, m/z) $[M]^+$ calcd for $C_{50}H_{86}O_2S_2$ 782.6148 measured 782.6074

IV-4-5. Synthesis of ,6-Bis(trimethyltin)-4,8-bis(2-octyldodecyloxy) benzo[1,2-*b*:3,4-*b′*]dithiophene (26)

To a solution of **25** (4 g, 5.1 mmol) in anhydrous THF (35 mL) was added dropwise to *n*-butyllithium(2.5 M in hexane, 8.16 mL, 20.4 mmol) via syringe at -78 °C under nitrogen atmosphere. The mixture was stirred at -78 °C for 30 min and then at room temperature for 30 min. After the mixture was cooled to -78 °C again, trimethyltin chloride (25.5 g, 25.5 mmol) was added. The mixture was warmed to room temperature and stirred for 12 h. After quenching the reaction with water, the volatile species were evaporated in vacuo. The residue was extracted with hexane, and the organic layer was washed with brine, dried over anhydrous MgSO4, and concentrated. The crude product was purified by recrystallization from methanol to yield as a colorless crystals (5 g, 4.51 mmol, 88%). Mp 38.5 – 38.7 °C ; ^{1}H NMR (300 MHz, $CDCl_3$) δ 7.41 (s, 2H), 4.08 (d, 4H, *J* = 5.21 Hz), 1.68 - 1.76 (m, 2H), 1.64 - 1.54 (m, 4H), 1.52-1.26 (m, 60H), 0.94-0.86 (m, 12H). ^{13}C NMR (75 MHz, CDCl3) δ 143.47, 140.56, 134.08, 133.13, 128.20, 39.43, 32.18, 31.61, 30.42, 30.00, 29.96, 29.93, 29.65, 29.61, 27.31, 22.93, 14.37 HRMS(FAB^{+}, m/z) $[M]^{+}$ calcd for C56H102O2S2Sn2 1110.5374 measured 1110.5370

IV-5. Synthesis of donor monomer

IV-5-1. Synthesis of 3,3'-Dibromo-2,2'-bithiophene (28)

To a solution of 2,3-dibromothiophene **(27)** (5 mL, 45.26 mmol) in dry ether (200 mL) was added to a 1.6 M solution of n-BuLi in hexane (29.4 mL, 47.07 mmol) dropwise at -78°C After stirring at -78°C for 1h,CuCl2 (9.13 g, 67.89 mmol) was introduced to the solution in one portion. The reaction mixture was stirred at -78°C for 2 h and then at room temperature for 2 days. The reaction mixture was quenched by 5 M HCl (500 mL) at 0°C and then extracted with chloroform three times (450 mL). The organic layer was dried over $MgSO_4$. After removal the solvent under reduced pressure, the residue was purified by column chromatography on silica gel (hexane) to give a yellow crystal 9 (6.5 g, 20.06mmol, 44.32 %)

IV-5-2. Synthesis of 3,3'-Di-n-octylsilylene-2,2'-bithiophene (29)

To a 1L 3-necked round bottom containing 28.84 mL (46.14 mmol) of 1.6 M n-butyllithium (caution!) in hexanes and 350 mL of THF at –78°C was added dropwise over 15 minutes to 6.5 g (20.06 mmol) of 3,3'-dibromo-2,2'-bithiophene (**16**) dissolved in 44.2 mL of THF. Immediately following this addition 7.18 g (36.09 mmol) of dichlorodi-n-octylsilane in 44.2 mL THF was

added dropwise over 30 minutes. After the addition was complete the reaction was quickly warmed to room temperature by placing the flask in a water bath. The mixture was stirred for 1 hour at this temperature then 200 mL of concentrated ammonium chloride was added to the reaction mixture. The mixture was poured into an addition funnel and 200 mL of hexanes was added. The organic layer was collected and the aqueous layer was further extracted with 3 x 100 mL of hexanes. The combined organic layers were dried over anhydrous MgSO4. The solvent was removed by rotary evaporation and the crude material was purified via flash chromatography using hexanes as the eluent yielding 3g (7.16mmol, 35.71%) of a pale yellow oil.

IV-5-3. Synthesis of 5,5'*Bis*(trimethylstannyl)-3,3'-Di-n-dodecylsilylene-2,2'-bithiophene (30)

To a solution of 2.20 g (4.14 mmol) of **7** in 50 mL of THF was added to 5.7 mL (9.1 mmol) of 1.6 M n-butyllithium (caution!) in hexane at –78°C. This was allowed to warm to room temperature and stirred at this temperature for 1 hour leading to the formation of a thick suspension. This was then susbsequently cooled to –78°C where a solution of 2.00 g (10.3 mmol) of trimethyltin chloride in 25 mL of THF was added dropwise. The reaction was warmed to room temperature and stirred overnight. The mixture was poured into a separation

funnel containing 200 mL DI water. To this was added 300 mL of hexane and the organic layer was separated. The organic layer was further washed with 5 x 100 mL DI water. The organic layer was dried over anhydrous MgSO4 and decolorized with activated charcoal. The mixture was filtered and the solvent was removed via rotary evaporation. The product was further dried by pulling vacuum on a high vac line for 48 hours yielding 3.4 g (95.7 %) of pale green oil. Attempts to further purify via chromatography with silica or alumina led to significant decomposition. 1H NMR (500 MHz, CD2Cl2): = 7.14 (m, 2H), 1.46-1.38 (m, 4H), 1.38- 1.15 (m, 36H), 0.92-0.83 (m, 10H), 0.39 (m, 18H). 13C NMR (125 MHz, CD2Cl2): = 155.43, 143.87, 138.55, 138.46, 33.87, 32.58, 30.34, 30.31, 30.23, 30.02, 29.86, 24.89, 23.35, 14.54, 12.65, -7.83. 119Sn NMR (184 MHz, CD2Cl2): = -27.28 (1*J*SnC = 184 Hz).

IV-6. Synthesis of donor monomer

IV-6-1. Synthesis of 2,7-dibromofluorene (32)

To a mixture of fluorene (10 g, 60.16 mmol), iodine (0.016 g, 0.001 mol), and CH_2Cl_2 (100 mL), bromine (6.23 mL, 121.52 mmol) diluted with CH_2Cl_2 (20 mL) were added dropwisely at 0 °C over a period of 1 h. After 12 h, a solution

of sodium bisulfite (3.0 g) in water (20 mL) was added and the mixture was stirred for 30 min to become colorless. The organic phase was separated and washed with water (150 mL). The organic phase was dried over anhydrous $MgSO_4$ and CH_2Cl_2 was distilled off. The product slurry was filtered and the product was dried under vacuum. A white solid 15.28 g. ^{1}H NMR (500 MHz, $CDCl_3$). δ (ppm): 7.62 (s, 2H), 7.58 (d, 2H), 7.48 (d, 2H), 3.83 (d, 2H).

IV-6-2. Synthesis of 2,7-Dibromo-9,9'-bis(2-ethylhexyl)fluorene (33)

To a solution of 2,7-dibromofluorene (10 g, 30.86 mmol) and tetrabutylammonium bromide (0.12 g, 0.52 mmol) in DMSO (70 mL), (2-ethylhexyl)bromide (13.72 g, 77.15 mmol) were added. The mixture was stirred at 80 °C for 2 h and then poured into water (100 mL). The mixture was extracted two times with diethyl ether and the combined organic phases were washed with brine, water and dried over Na_2SO_4. Upon evaporating off the solvent the residue was purified via column chromatography with n-hexane as eluent to afford a colourless oil, which was recrystallized from ethanol at -20 °C to afford colourless crystals (90.6%). ^{1}H NMR (400 MHz, $C_2D_2Cl_4$, 25 °C): δ = 7.53-7.39 (m, 6H, Ar-H), 1.91 (d, 4H, J =5.7 Hz, Ar- CH_2), 1.00-

0.35 (m, 30H, Alkyl-H) ppm. ^{13}C NMR (100 MHz, $C_2D_2Cl_4$, 25 °C): δ = 152.4, 139.1, 130.0, 127.4, 121.0, 120.9, 55.3, 44.3, 34.7, 33.5, 28.0, 27.0, 22.7, 13.9, 10.3 ppm. LR-MS (EI, m/z): 41 (23.7), 43 (40.6), 57 (100.0), 71 (29.5), 141 (17.0), 176 (11.6), 546 (23.8), 548 [M^+] (45.7), 549 (14.2), 550 (23.8).

IV-6-3. Synthesis of 2,2'-(9,9-Bis(n-propyl)-fluoren-2,7-diyl)-bis[4,4,5,5-tetramethyl-[1,3,2]dioxaborolane] (34)

A solution of 2,7-dibromo-9,9-bis(n-propyl) fluorene (3 g, 5.32 mmol) in anhydrous THF (50 ml) was added to n-BuLi (1.6 M in hexane, 7.32 ml) at -78°C. The reaction mixture was stirred for 1 h before 2-isopropoxy-4,4,5,5-tetramethyl-[1,3,2]dioxaborolane (2.53 ml, 12.79 mmol) was added in one portion. The mixture was warmed to room temperature, stirred overnight and poured into a large amount of water for extraction with methylene chloride. The organic exracts were washed with brine and dried over $MgSO_4$. Upon evaporating off the solvent, the residue was recrystallized with acetone to yield 2a (0.680 g, 44%) as a white crystal. 2,2' -(9,9-Bis(2-ethylhexyl-fluoren-2,7-diyl))-bis[4,4,5,5-tetramethyl-[1,3,2]dioxaborolane] Column

chromatography on silica gel with petroleum ether:methylene chloride (2:1) as the eluent afforded **34** as a white crystal in a 52 % yield. ^{1}H-NMR (400 MHz, $CDCl_3$): δ (ppm) 7.82-7.87 (m, 2H), 7.80 (dd, J = 7.50 Hz, 0.79 Hz, 2H), 7.73 (d, J = 7.40 Hz, 2H), 2.02 (d, J = 5.32 Hz, 4H), 1.39 (s, 24H), 0.65-0.91 (m, 24H), 0.47-0.53 (m, 6H).

IV-7. Synthesis of donor monomer

IV-7-1. Synthesis of 4,4'-Dibromo-2-nitrobiphenyl (36)

A mixture of fuming HNO_3 (16.82 mL) and AcOH (150 mL) was added portionwise to a suspension of 4,4'-Dibromobiphenyl (5 g, 16.02 mmol). Over the course of the addition, the reaction turned increasingly orange and warmed slightly, and the solid began to dissolve. After 18 h, the reaction had darkened considerably, and TLC showed complete disappearance of the starting material. The reaction was poured into H_2O (1.4 L) containing NaOH (35 g) to partially neutralize the acid, resulting in the formation of a tacky yellow precipitate. The mixture was divided into two equal volumes that were each in turn extracted with CH_2Cl_2 (4 x 75 mL). The combined organic layers (600 mL) were washed vigorously with H_2O (3 x 100 mL) and brine, dried over

$MgSO_4$, and concentrated in vacuo to a yellow solid. MeOH (300 mL) was added, the solvent stripped to form a thick slurry (approx 25-50 mL MeOH remaining), and subsequently filtered. The pale yellow solid was washed with ice cold MeOH (100 mL) and dried to give 4,4'-Dibromo-2-nitrobiphenyl, yield 5.58 g, 93%. ^{1}H NMR ($CDCl_3$) δ 7.16 (ABq, 2H), 7.28 (d, J = 8 Hz, 1H), 7.56 (ABq, 2H), 7.75 (dd, J = 2 Hz, 8 Hz, 1H), 8.02 (d, J = 2 Hz, 1H).

IV-7-2. Synthesis of 2,7-Dibromocarbazole (37)

The 100 mL of triethyl phosphate solution of **36** (5.58 g, 15.93 mmol) was stirred under nitrogen at 150 °C for 3 h. After cooled to the room temperature, the solvent was poured into deionized water and extracted with dichloromethane to give **37**. Yield 1.16 g, 22.1%, white solid. ^{1}H-NMR ($CDCl_3$, 600 MHz) δ: ppm 8.07 (s, 1H), 7.87 (d, 2H), 7.51 (m, 2H), 7.31 (t, 2H).

IV-7-3. Synthesis of octylmagnesium bromide (39)

A 1L three-necked round-bottom flask equipped with a magnetic stirring bar, reflux condenser, addition funnel, and a thermometer was charged with magnesium turnings (6.18 g, 256.30 mmol). The flask was gently heated under argon atmosphere (50 °C), while the magnesium turnings were vigorously stirred

for 1 h affording activation of the magnesium surface. After cooling to 25 °C and addition of THF (50 mL), 10 mL of a solution of octyl bromide 30 mL, 170.87 mmol) in THF (40 mL) was added to the suspension while continously stirring. The reaction started after 2-3 min as indicated by a small rise in temperature. Thereafter, the remaining solution of OctBr was added dropwise over a periode of 4 h while keeping the temperature below 30 °C. After stirring the reaction mixture for additional 2 h, the supernatant solution was then cannulated into a new dry, argon-flushed Schlenk flask and titrated with iodine affording the concentration of active octylmagnesium bromide.

IV-7-4. Synthesis of Heptadecan-9-ol (40)

To a mixture solution of ethyl formate (3.47 mL, 42.72 mmol) and anhydrous THF (22 mL) in a three-necked flask under nitrogen stirred at -78°C, *n*-octylmagnesium bromide [40.3 mL, 80.5 mmol] was added slowly, and the mixture was stirred for 24 h. Then, the mixture was quenched by methanol and saturated aqueous NH_4Cl, extracted with ether three times, washed by saturated aqueous NaCl, and dried over anhydrous $MgSO_4$. After evaporation, white solid was obtained with the yield of 18 % (7.15g). 1H NMR (270 MHz, CDCl3, ppm) : δ 3.58 (m, 1H) , 1.42 (m, 8H) , 1,27 (m, 21H) , 0.88 (t, J = 6.8 Hz, 6H).

IV-7-5. Synthesis of 9-Heptadecane p-toluenesulfonate (41)

To a mixture of heptadecan-9-ol (2 g, 7.80 mmol), CH_2Cl_2 (70 mL), Me_3NHCl (0.75 g, 7.8 mmol), and Et_3N (2.83 mL, 20.208 mmol) in a three-necked flask under nitrogen stirred at 0 oC, TsCl (1.94 g, 10.14 mmol) was added slowly, and the mixture was stirred for 90 min at 0°C. Then, the mixture was quenched by water, extracted with CH2Cl2 three times, washed by water, saturated aqueous NaCl, and dried over anhydrous Na_2SO_4. After evaporation and purification by column chromatography (n-hexane : ethyl acetate = 1 : 9), opaque crystals were obtained with the yield of 52.95 % (1.77 g). 1H NMR (270 MHz, $CDCl_3$, ppm) : δ 7.79 (d, J = 8.1 Hz, 2H) , 7.32 (d, J = 8.1 Hz, 2H) , 4.53 (qt, J = 5.9 Hz, 1H) , 2.44 (s, 3H) , 1.56 (m, 4H) , 1.22 (m, 24H) , 0.88 (t, J = 6.8 Hz, 6H).

IV-7-6. Synthesis of 2,7-Dibromo-9-(heptadec-9-yl)carbazole (42)

A solution of toluene-4-sulfonic acid heptadec-9-yl ester **(41)** (3.7 g, 5.63 mmol) in DMSO (45 mL) was added dropwise over 1 h to mixture of 2,7-dibromo-9-H-carbazole **(37)** (1.83 g, 5.63 mmol), freshly powdered KOH (1.58 g, 28.15 mmol) and DMSO (45 mL) at room temperature. Upon complete addition the mixture was stirred at room temperature for 6 h then poured into water (200 mL) and the aqueous layer extracted with hexane (100 mL). The combined organic fractions were washed with brine (100

cm3), dried (MgSO4), filtered and concentrated under reduced pressure. Purification was carried out via column chromatography to yield a white crystalline solid (2.03 g, 63.99%). 1H NMR (CDCl3) dH: 0.83 (6H, t, J ¼ 6.8 Hz), 1.13–1.26 (36 H, m), 1.90 (2H, quart), 2.20 (2H, quart), 4.41 (1H, quint), 7.32 (2H, broad m), 7.53 (1H, broad s), 7.69 (1H, broad s), 7.90 (2H, broad m). MS m/z (EI): 565, 563 (Mþ), 561.

IV-7-7. Synthesis of 2,7-Bis(4',4',5',5'-tetramethyl-1',3',2'-dioxaborolan-2'-yl)-*N*-9"-heptadecanylcarbazole (43)

To a mixture of *N*-9'-heptadecanyl-2,7-dibromocarbazole (2 g, 3.55 mmol) and anhydrous THF (20 mL) in a three-necked flask under nitrogen stirred at -78℃, *n*-BuLi [6.66 mL (1.6 M in hexane)] was added slowly, and the mixture was stirred for 6 h at -78℃ To a mixture, 2-isopropoxy-4,4,5,5,-tetramethyl-1,3,2-dioxaborolane (2.45 mL, 12.42 mmol) was added and stirred for 2 h. Afterward the mixture was allowed to warm up to room temperature and stirred for 24 h. Then, the mixture was quenched by water, extracted with ether three times, washed by water, saturated aqueous NaCl, and dried over anhydrous MgSO4. After evaporation and purification by column chromatography (*n*-hexane : ethyl acetate = 15 :1) and recycling HPLC, opaque solid were obtained with the yield of 60 % (1.4 g). 1H NMR (270 MHz, CDCl3, ppm) : δ 8.13 (t, *J* = 8.4 Hz, 2H) ,

8.02 (s, S6 1H) , 7.89 (s, 1H) , 7.66 (d, J = 5.4 Hz, 2H) , 4.70 (t, J = 5.0 Hz, 2H) , 2.33 (m, 2H) , 1.90 (m, 2H) , 1.61 (m, 2H) , 1.39 (s, 24H) , 1.19 (br, 24H) , 0.98 (br, 2H) , 0.87 (t, J = 6.4 Hz, 6H).

IV-8. Synthesis of polymer

IV-8-1. Synthesis of Poly-(5-(4,8-bis(octyloxy)-6-phenylbenzo[1,2-b:4,5-b']dithiophen-2-yl))-6,7-difluoro-2,3-dihexyl-8-phenylquinoxaline (YJ-6)

Carefully purified 5,8-Dibromo-6,7-difluoro-2,3-dihexylquinoxaline **(9)** (0.4 g, 0.8126 mmol) , 6-Bis(trimethyltin)-4,8-bis(2-octyldodecyloxy)benzo[1,2-*b*:3,4-*b'*]dithiophene **(26)** (0.628 g, 0.8126 mmol) , P(*o*-tolyl)$_3$ (40 mol%) and $Pd_2(0)$ $(dba)_3$ (5 mol%) were dissolved in a mixture of chlorobezene. The mixture was refluxed with vigorous stirring for 8 hr under argon atmosphere. After 36 hr, phenyltributylstannane was added to the reaction then 8 hr later, bromobenzene was added and the reaction mixture refluxed overnight to complete the end-capping reaction. The whole mixture was poured into methanol. The resulted solid was filtered and washed with acetone to remove oligomers and catalyst residues. **YJ-6**, these polymer was soluble in conventional organic solvents (toluene, chloroform, and THF).

IV-8-2. Synthesis of 5-(4,4-bis(2-ethylhexyl)-6-methyl-4H-cyclopenta[1,2-b:5,4-b']dithiophen-2-yl)-6,7-difluoro-2,3-dihexyl-8-methylquinoxaline(YJ-7)

Carefully purified 5,8-Dibromo-6,7-difluoro-2,3-dihexylquinoxaline **(9)** (0.5 g, 1.24mmol) , 4,4-Di(2-ethtylhexyl)-4H-cyclopenta[2,1-b:3,4-b(]dithiophene **(20)** (0.61 g, 1.24 mmol) , K_2CO_3(150 mol%) and $Pd(OAc)_2$ (5 mol%) were dissolved in a mixture of Dimethylacetamide. The mixture was refluxed with vigorous stirring for 24 hr under argon atmosphere. The whole mixture was poured into methanol. The resulted solid was filtered and washed with acetone to remove oligomers and catalyst residues. **YJ-7**, these polymer was soluble in conventional organic solvents (toluene, chloroform, and THF).

IV-8-3. Synthesis of 6,7-difluoro-2,3-dihexyl-5-methyl-8-(6-methyl-4,4-dioctyl-4H-silolo[3,2-b:4,5-b']dithiophen-2-yl)quinoxaline (YJ-8)

Carefully purified 5,8-Dibromo-6,7-difluoro-2,3-dihexylquinoxaline **(9)** (0.54 g, 1.098 mmol) , 5,5'*Bis*(trimethylstannyl)-3,3'-Di-n-dodecylsilylene-2,2'-bithiophene **(30)** (0.800 g, 1.098 mmol) , P(*o*-tolyl)$_3$ (40 mol%) and $Pd_2(0)(dba)_3$ (5 mol%) were dissolved in a mixture of chlorobezene. The mixture was refluxed with vigorous stirring for 8 hr under argon atmosphere. After 36 hr, phenyltributylstannane was added to the reaction then 8 hr later, bromobenzene

was added and the reaction mixture refluxed overnight to complete the end-capping reaction. The whole mixture was poured into methanol. The resulted solid was filtered and washed with acetone to remove oligomers and catalyst residues. **YJ-8**, these polymer was soluble in conventional organic solvents (toluene, chloroform, and THF).

IV-8-4. Synthesis of 5-(5-(4,8-bis(octyloxy)-6-phenylbenzo[1,2-b:4,5-b']dithiophen-2-yl)thiophen-2-yl)-6,7-difluoro-2,3-dihexyl-8-(5-phenylthiophen-2-yl)quinoxaline (YJ-9)

Carefully purified 5,8-bis(5-bromothiophen-2-yl)-6,7-difluoro-2,3-dihexylquinoxaline**(13)** (0.55 g, 0.838 mmol) , 6-Bis(trimethyltin)-4,8-bis(2-octyldodecyloxy)benzo[1,2-*b*:3,4-*b'*]dithiophene **(26)** (0.647 g, 0.838 mmol) , P(*o*-tolyl)$_3$ (40 mol%) and $Pd_2(0)(dba)_3$ (5 mol%) were dissolved in a mixture of chlorobezene. The mixture was refluxed with vigorous stirring for 8 hr under argon atmosphere. After 36 hr, phenyltributylstannane was added to the reaction then 8 hr later, bromobenzene was added and the reaction mixture refluxed overnight to complete the end-capping reaction. The whole mixture was poured into methanol. The resulted solid was filtered and washed with acetone to remove oligomers and catalyst residues. **YJ-9**, these polymer was soluble in conventional organic solvents (toluene, chloroform, and THF).

IV-8-5. Synthesis of 5-(5-(9,9-bis(2-ethylhexyl)-7-phenyl-9H-fluoren-2-yl)thiophen-2-yl)-6,7-difluoro-2,3-dihexyl-8-(5-phenylthiophen-2-yl)quinoxaline (YJ-10)

Carefully purified 5,8-bis(5-bromothiophen-2-yl)-6,7-difluoro-2,3-dihexylquinoxaline**(13)** (0.599 g, 0.9124 mmol) , 2,2'-(9,9-Bis(n-propyl)-fluoren-2,7-diyl)-bis[4,4,5,5-tetramethyl-[1,3,2]dioxaborolane] **(34)** (0.586 g, 0.9124 mmol) , K_2CO_3 (1.261 g, 9.124 mmol) and $Pd(PPh_3)_4$ (3 mol%) were dissolved in a mixture of chlorobezene. The mixture was refluxed with vigorous stirring for 8 hr under argon atmosphere. After 36 hr, phenylboronic acid was added to the reaction then 8 hr later, bromobenzene was added and the reaction mixture refluxed overnight to complete the end-capping reaction. The whole mixture was poured into methanol. The resulted solid was filtered and washed with acetone to remove oligomers and catalyst residues. **YJ-10**, these polymer was soluble in conventional organic solvents (toluene, chloroform, and THF).

IV-8-6. Synthesis of 2-(5-(6,7-difluoro-2,3-dihexyl-8-(5-phenylthiophen-2-yl)quinoxalin-5-yl)thiophen-2-yl)-9-(heptadecan-9-yl)-7-phenyl-9H-carbazole (YJ-11)

Carefully purified 5,8-bis(5-bromothiophen-2-yl)-6,7-difluoro-2,3-

dihexylquinoxaline**(13)** (0.599 g, 0.9124 mmol) , 2,7-Bis(4',4',5',5'-tetramethyl-1',3',2'-dioxaborolan-2'-yl)-*N*-9"-heptadecanylcarbazole **(43)** (0.600 g, 0.9124 mmol) , K_2CO_3 (1.261 g, 9.124 mmol) and $Pd(PPh_3)_4$ (3 mol%) were dissolved in a mixture of chlorobezene. The mixture was refluxed with vigorous stirring for 8 hr under argon atmosphere. After 36 hr, phenylboronic acid was added to the reaction then 8 hr later, bromobenzene was added and the reaction mixture refluxed overnight to complete the end-capping reaction. The whole mixture was poured into methanol. The resulted solid was filtered and washed with acetone to remove oligomers and catalyst residues. **YJ-11**, these polymer was soluble in conventional organic solvents (toluene, chloroform, and THF).

References

[1] J. H. Zhao, A. H. Wang, M. A. Green and F. Ferrazza, Appl. Phys. Lett., 1998, 73, 1991–1993.

[2] R. F. Service, Science, 2011, 332, 293.

[3] Y. Li and Y. Zou, Adv. Mater., 2008, 20, 2952–2958.

[4] X. Zhan and D. Zhu, Polym. Chem., 2010, 1, 409–419.

[5] S. C. Price, A. C. Stuart, L. Q. Yang, H. X. Zhou and W. You, J. Am. Chem. Soc., 2011, 133, 4625–4631.

[6] Y. Y. Liang and L. P. Yu, Acc. Chem. Res., 2010, 43, 1227–1236.

[7] Chunhui Duan, Fei Huang* and Yong Cao (2010), J. Mater. Chem., 2012, 22, 10416

[8] Krebs, F. C., et al., *J Mater Chem* (2009) 19(30), 5442-5451.

[9] Irwin, M. D., *et al.*, *P Natl Acad Sci USA* (2008) 105(8), 2783.

[10] Olthof, S., *et al.*, *Phys Rev B* (2009) 79(24).

[11] Nelson, Jenny, Materials Today (Oxford, United Kingdom), (2011), 14(10), 462-470

[12] Muhlbacher, D., *et al.*, *Adv Mater* (2006) 18(21), 2884.

[13] Bronstein, H., *et al.*, *J Am Chem Soc* (2011) 133(10), 3272.

[14] Li, G., Chu, C.-W., Shrotriya, V., Huang, J. & Yang, Y. Appl. Phys. Lett. 88, 253503 (2006).

[15] Huo, L. et al. Macromolecules 42, 6564–6571 (2009).

[16] Letian Dou, Yang Yang, NATURE PHOTONICS, 2012, 6, 180-185.

[17] He, Y. J., Chen, H.-Y., Hou, J. H. & Li, Y. F. J. Am. Chem. Soc. 132, 1377–1382 (2010).

[18] Chou, C. H. et al. Adv. Mater. 23, 1282–1286 (2011).

감사의 글

길고도 짧은 석사 생활 2 년이 지나갔습니다. 수많은 일들이 있었고 그로 인해 더 많이고 성장할 수 있었던 계기가 되었습니다. 늘 저를 응원해 주시고 걱정해주신 모든 분들께 감사 드립니다.

제일먼저 지도교수님 이신 진영읍 교수님께 감사 드립니다. 학부시절부터 실험실 생활을 하면서 실험실을 만들어가며 많은 정을 느낄 수 있었고 가족 같은 실험실 원들과 시작을 다 같이 했다는 것에 보람을 느낍니다. 화가 나고 힘들 때마다 서로를 의지하고 무엇이든지 함께 풀어 나가면서 시너지 효과를 낼 수 있게끔 분위기를 이끌어 주셔서 감사 드립니다. 그리고 논문 심사를 봐주신 박성수 교수님과 이근대 교수님께도 감사 드립니다. 저희를 보실 때마다 칭찬과 힘을 실어 주시는 좋은 말씀을 많이 해주셔 늘 존경해 왔습니다. 그리고 먼저 졸업한 해심이 누나! 제가 말도 잘 안 듣고 몇 번을 울렸지만 늘 챙겨주시고 졸업해서도 취업에 관한 많은 이야기와 영어에 관한 도움은 정말 감사합니다. 누나와 석사생활을 할 때 울고 웃던 많은 일들은 늘 떠올리면서 누나가 졸업을 해도 술자리에서 많이 이야기를 했었습니다. 제가 취직하면 꼭 전주에 놀러 간다고 했던 약속 꼭 지키겠습니다. 지금은 정신이 없고 적응도 필요하니까 올해가 지나가기 전에는 꼭 갈게요. 맛있는 거 많이 사주세요!!! 그리도 동호행님! 행님한테도 매일 까불고 버릇없이 굴어도 가끔은 화를 내시지만 늘 참고 동생이라 챙겨주셔서 감사합니다. 집에 자주 초대해주고 맛있는 음식도 주셔서 감사해요! 행님이 아니고 형수님께 감사해야겠네요. 제가 형수님과 조카는 따로 챙기겠습니다. 그리고 석사는 한 학기 선배지만 많은 것을 가르쳐 주지 못한 것도 죄송해요! 더 많은 것을 가르쳐 드리고 했었어야 했는데 짐만 더 드리고 가는 건지 모르겠네요. 하여튼 행님도 남은 6 개월 준비 잘 하셔서 좋은 논문이랑 취업했으면 합니다. 그리고 경훈이행님! 그렇게 오랜 시간을 보내지는 못했지만 그래도 많은 정이 들었던 것 같아요. 행님 역시 졸업하시고 떠나셨어도 늘 생각하고 술자리에서 이야기하곤 했습니다. 그래도 늘 연락해 주시고 격려해주셔서 감사합니다. 그리고 여자친구 사귀신 것 축하 드리고 서울에 데이트 장소 좀 가르쳐 주세요. 서로 공유해요! 다음으로 원준이~ 비록 6 개월 같이 지냈지만 친구가 들어와서 많은 힘이 되어 줬던 것 같다. 같이 집에

걸어가면서 힘들거나 걱정거리 다 들어주고 격려해줘서 고맙다. 막내로 들어와서 힘든 일들 다 혼자서 하고 도움을 못 줘서 미안하고 많은 것을 가르쳐 주지 못해서 미안하다. 근데 잘 할 것 같다. 유기화학에 관심도 많고 지식도 많으니까 좋은 물질도 많이 합성하고 좋은 논문도 많이 쓸 수 있을 것 같다. 인제 니가 에이스자나~! 열심히 하고 아니까 좋은 결과 있을 꺼다~!! 힘내고 열심히 하자!
그리고 동기 이지만 늘 저의 방장이신 은준이 행님! 힘들게 처음부터 같이 지내오면서 행님한테는 진짜 많이 배웠습니다. 실험적인 것뿐만 아니라 사람을 대하는 것 등 많은 것을 배웠습니다. 행님 아니었으면 조기졸업은 생각도 안 했을 겁니다. 행님 하신다 길래 조기졸업도 선택했고 처음 들어온 동기들 다 대학원을 진학 하지 않아도 행님한테 들었던 많은 이야기들을 통해 대학원진학에 마음을 굳힐 수 있었던 것 같아요. 제 물질도 행님의 도움이 많이 컸습니다. 늘 감사하게 생각합니다. 제가 먼저 취직해서 떠나지만 행님은 저보다 더 뛰어나시니깐 더 좋은 곳에 취직할 수 있을 것이라고 생각합니다. 늘 감사하게 생각합니다. 그리고 민성이~몇 일 보지도 못했네. 그래도 우리 실험실에 와서 반갑고 관심이 있어서 왔으니까 원준이한테 많이 배워서 잘 지내고, 난 자주 부산 갈 거니까 자주 보자! 그리고 부산대 식구들 정말 감사합니다. 송박사님, 주영이 누나, 주애 누나, 수연이 그 외 많은 분들 감사합니다. 같은 실험실은 아니지만 늘 챙겨주시고 모르는 부분은 가르쳐주시고 부산대 식구들에게도 정이 많이 들었네요. 매일 필요할 때만 연락 드린 것 같아 죄송합니다. 제가 한번 찾아가서 꼭 감사함을 전하겠습니다. 그리고 진욱이 행님, 주호, 현정이 늘 맛있는 것 나눠먹고 챙겨주고 해서 감사합니다. 고마움은 절대 잊지 않을게요.
마지막으로 혼자 자취하는 아들 뒷바라지 한다고 고생한 우리 엄마, 아빠, 누나, 매형 늘 내 지원군이 되어주고 나 짜증부리고 고민거리 다 받아주고 2년 기다려 줘서 너무 감사합니다. 매일 혼자 산다고 걱정하시는 엄마, 아빠! 인제 용돈도 안받아 갈게요! 그 동안 고생 많았습니다. 이제 아들 노릇 많이 할 테니 항상 건강하세요. 그리고 우리 누나, 매형. 늘 응원해주고 걱정해주고 챙겨줘서 고맙습니다. 인제 내가 챙겨주고 할게요! 늘 감사합니다. 사랑합니다 내 가족들♥ 마지막으로 학교 선배들, 후배들, 행님 누나들! 항상 절 믿어주고 아낌 없는 지원 너무 감사합니다~!! 이 은혜 절대 잊지 않을게요! 진짜 마지막으로 2년동안 큰 힘이 되어준 여자친구 희주야~고맙다.♥
정말 감사합니다.